Photoactivated Artificial Molecular Machines that Can Perform Tasks

Photo-activated artificial molecular machines that can perform tasks

Stefano Corra, Massimiliano Curcio, Massimo Baroncini, Serena Silvi and Alberto Credi*

Dedicated to Vincenzo Balzani on his 83th birthday

Dr. S. Corra, Dr. M. Curcio, Dr. M. Baroncini, Prof. Dr. A. Credi

Dipartimento di Scienze e Tecnologie Agro-alimentari, Università di Bologna

Viale Fanin 44, 40127 Bologna, Italy

E-mail: alberto.credi@unibo.it

Prof. Dr. S. Silvi

Dipartimento di Chimica "G. Ciamician", Università di Bologna

Via Selmi 2, 40127 Bologna, Italy

Abstract: Research on artificial photo-activated molecular machines has moved in recent years from a basic scientific endeavor towards a more applicative effort. Nowadays, the prospect of reproducing the operation of natural nanomachines with artificial counterparts is no longer a dream but a concrete possibility. This review illustrates the progress towards the construction of molecular machine-based devices and materials in which light irradiation results in the execution of a task as a result of nanoscale movements. After a brief description of a few basic types of photo-activated molecular machines, significant examples of their exploitation to perform predetermined functions are presented. These include switchable catalysts, nano-actuators that interact with cellular membranes, transporters of small molecular cargos, and active joints capable of mechanically coupling molecular-scale movements. Investigations aimed at harnessing the collective operation of a multitude of molecular machines organized in arrays to perform tasks at the microscale and macroscale in hard and soft materials are also reviewed. Surfaces, gels, liquid crystals, polymers, and self-assembled nanostructures are described wherein the nanoscale movement of embedded molecular machines is amplified, allowing the realization of muscle-like actuators, microfluidic devices, and polymeric materials for light energy transduction and storage.

Keywords: Azobenzene, Nanoscience, Photochemistry, Rotaxane, Supramolecular Chemistry

1. Introduction

Molecular machines are molecular-based species in which the stimulation with an energy input causes the controlled and directed movement of some of their (sub)components with respect to the others.[1] The most outstanding examples of molecular machines are found in living organisms, where motor proteins such as myosin, kinesin and ATP synthase operate efficiently in complex environments, tasked with functions of crucial importance for life.[2,3,4] The existence of biomolecular machines highlights the relevance of nanoscale devices in the natural world, and motivates research efforts to realize artificial analogues, in the frame of the development of nanotechnology.

During the past three decades, chemists have designed, synthesized and investigated a large variety of molecular machines and motors based on the stimulation of appropriately designed molecular or supramolecular systems with chemical, electrical or photonic inputs.[1,5,6,7] Surely, the marriage of synthetic, physical and analytical chemistry with an engineering mentality has led to ingenious achievements.[8] More importantly, significant progress has been made in understanding controlled motion at the nanoscale, that is, how molecular-sized objects can exploit an energy source to move directionally in an environment dominated by the incessant and random thermal agitation.[9] The maturity, scientific value and potential for application of this research field has been recognized by the award of the Nobel Prize in Chemistry 2016 ‘for the design and synthesis of molecular machines’.[10,11,12]

As it happens for the macroscopic counterparts, important properties of a molecular machine are the type of energy supplied to make it work and the way in which its operation is monitored. Light can indeed fulfil both roles. A photon absorbed by a molecule provides it with electronic energy, and a reaction that would be endoergonic in the dark may take place. The structural and/or electronic changes caused by the transformation are reflected in the modification of the physico-chemical properties of the system, often including its optical

response. Therefore, photons can be used both for 'writing' and 'reading' molecular machines. Detailed discussions on the use of light to operate artificial molecular machines, and on the types of photoinduced processes that may be exploited for this purpose, can be found in the literature.[13,14,15,16,17]

It is worth noting that in nature the direct conversion of solar radiation into mechanical work is a rare event; rather, light energy is converted through photosynthetic processes to produce chemical fuels such as the ATP that powers motor proteins.[18] Researchers, however, do not necessarily need to follow nature's blueprint.[19] The development of light-activated molecular machines is not only scientifically appealing but also deeply justified from a societal standpoint. In order to face the stringent problems of energy supply and climate change, it is clear that the products of a future nanotechnology-based industry will have to be powered by renewable and clean energy sources. In this frame, the construction of molecular machines capable of utilizing sunlight to produce mechanical work is certainly an interesting option.

A distinctive feature of biological nanomachines is that molecular motion is harnessed to execute useful tasks at different length scales. They include, for example, the making of other molecules (nanoscopic scale), intracellular transport of objects (microscopic scale), and muscle-type actuation and locomotion (macroscopic scale).[2-4] Until about ten years ago, despite the high level of sophistication already reached in the design, synthesis and investigation of artificial molecular machines powered by light, convincing evidence that such nanodevices can deliver on their promise – that is, perform useful tasks in the real world – was essentially missing.[20] This scenario has started to change in recent years, when experiments suggesting that synthetic molecular machines could provide the bases for ground-breaking applications in several areas of technology and medicine begun to appear.[17,21,22] In this article, we highlight the progress along this direction by presenting examples in which the photoinduced motion of synthetic molecular machines is harnessed, transmitted or collected

such that a sizeable effect that goes beyond the machine itself is achieved. After a brief description of the types of molecular machine employed for this purpose, the discussion is organized according to the kind of function enabled by the molecular movement.

2. Basic types of photochemically driven molecular machines

In this section we recall at a qualitative level the design, structural features and operation schemes of a few classes of artificial molecular machines in which light excitation causes rotatory or linear movements. For the sake of the discussion and for space reasons, we limit our examination to systems that are instrumental for describing the examples reported in the next sections. In-depth discussions on the mechanisms that enable controlled motion in molecular systems by exploiting an external energy source,[5-7,9,17] and comprehensive reviews of photochemically driven synthetic molecular machines[1,5-8,10-17] are available in the literature.

2.1 Molecular rotary motors

A rotary motor is a type of machine capable of using an energy input to perform repeated unidirectional 360-degrees rotations of one component of the device with respect to the other(s).[1,5,17] The construction of rotary motors at the molecular level is particularly challenging because it is difficult to fulfil the requirement of unidirectional rotation. Artificial photochemically driven molecular rotary motors have been first obtained by exploiting the light-induced isomerization around a C=C double bond in chiral overcrowded alkenes.[23] This class of molecular machines has evolved impressively over the past two decades,[10,21] and has been exploited in various settings to control functions (see the next sections).

The operation of overcrowded alkene rotary motors and the role of light can be conveniently described for the first prototype of the series, based on the symmetric biphenanthrylidene species **1** (**Figure 1**). In this compound, because of the steric encumbrance present in the

structure, the double bond system is forced out of planarity, giving a helical shape to the molecule. As each subunit can adopt a right-handed (*P*) or a left-handed (*M*) helicity, a total of four stereoisomers are possible for the (*R,R*) enantiomer of **1** (Figure 1a). The *E*-*Z* photoisomerization reactions are photochemically reversible and take place upon irradiation at appropriate wavelengths, whereas the helix inversion processes (while maintaining the *E* or *Z* configuration) are irreversible – that is, unidirectional – thermally activated processes. The rotation directionality in the helix inversion is determined by the energetic preference for the methyl substituents to adopt a less sterically demanding and energetically favorable axial orientation. As depicted in Figure 1b, a sequence of two energetically uphill light driven isomerization processes and two energetically downhill thermal helix inversion steps is responsible for the unidirectional 360° rotation. The continuous irradiation (≥280 nm) of this compound at a sufficiently high temperature (60°C) enables repeated rotations and thus the motor exhibits *autonomous* behavior, that is, it operates without external intervention – in other words, in a constant environment – as long as the energy source (light) is available.

<FIGURE 1>

Several species evolved from the parent compound **1** have been developed and extensively investigated,[10,21,24] and motors capable of rotating at room temperature with MHz frequencies upon visible light irradiation are now available. It was also shown that the light-driven unidirectional rotation is preserved when the motors are deposited on macroscopic[25] or nanostructured[26] surfaces, embedded in membranes,[27] and incorporated in soft[28] or hard[29] materials. Indeed, the robustness of the motor function is one of the main reasons for the widespread use of these compounds in the search for technological applications of artificial molecular machines. Light-driven rotary motors based on different classes of

molecules – for example, imines,[30] indigos,[31] and catenanes[32] – have also been investigated.

2.2 Rotaxane-based molecular shuttles and muscles

Molecular shuttles are rotaxanes in which the ring component can move in a linear fashion along a molecular axle endowed with terminal bulky groups to prevent dethreading.[33] Systems of this kind, that are reminiscent of an abacus, are probably the most popular implementation of the molecular machine concept with artificial chemical species.[1,5-8,13,15-17] The minimal design of a molecular shuttle in which the position of the ring along the axle can be controlled[34] involves the incorporation of two different recognition sites (stations) on the axle. The ring initially encircles the most efficient station (i.e., the one with the highest affinity for the ring) until a chemical reaction, triggered by a stimulus, changes the relative affinity between the ring and the stations, thereby causing the translation of the ring to the other station.

Light-triggered reactions such as photoinduced electron transfer[35,36,37] and photoisomerization[38,39,40,41] have been largely employed to modulate the interaction of the ring with the stations in order to cause mechanical movements. An interesting example of this kind is described in **Figure 2**.[42] A monolayer of the photoactive rotaxane *(E)*-**2**, which consists of a ferrocene-functionalized β-cyclodextrin (β-CD) macrocycle threaded on a molecule containing a photoisomerizable azobenzene unit and a long alkyl chain, was self-assembled on a gold electrode. The ring component is entrapped on the axle because of the presence of an anthracene stopper. The azobenzene unit in the *E* configuration is complexed by β-CD; upon photoisomerization to the *Z* form the encapsulation becomes sterically impossible, leading to a net displacement of the β-CD ring towards the alkyl spacer. Back $Z \rightarrow E$ photoisomerization triggers the return of the macrocycle at the original

location. As the current intensity associated with oxidation of the appended ferrocene unit depends on its distance from the electrode, the position of the β-CD ring along the axle could be determined electrochemically. Interestingly, this nanomechanical device exploits a shuttling motion to transduce optical information (light input) into an electrical signal (current output).

<FIGURE 2>

By relying on the combination of the controllable molecular shuttle concept with doubly interlocked rotaxane dimers ([c2]daisy chains), compounds that can undergo stimuli-induced contraction and extension movements have been developed.[43] Systems of this kind have been nicknamed 'molecular muscles' because of the functional resemblance with the sarcomeres present in skeletal muscles (see section 7).[44,45] For example, following the same switching principle of compound **2**, the rotaxane dimer **3** (**Figure 3**) can be reversibly interconverted between extended and contracted forms as a consequence of the *E*-*Z* photoisomerization of the stilbene units incorporated in the axles.[46] While stilbene in its *E* configuration is complexed by an α-cyclodextrin ring, isomerization to the *Z* form changes the preferred position of the macrocycle along the axle. Doubly interlocked [c2]daisy chain rotaxanes analogous to **3** and based on the *E*-*Z* photoisomerization of azobenzene have also been investigated.[47,48]

<FIGURE 3>

3. Catalysis

A major task of biomolecular machines is the synthesis of other molecules, achieved by the precise control of chemical reactions through complex catalytic effects.[2-4] An exciting goal for artificial molecular machines is indeed the exploitation of their movements to implement dynamic, stimuli-responsive catalytic effects.[49,50]

Molecular rotary motors of the overcrowded alkene type (section 2.1) have been employed to construct catalysts for enantioselective transformations, whose efficiency could be modulated by light irradiation. In fact, the individual chiral species formed during the unidirectional rotary cycle (Figure 2), combined with catalytic moieties in suitably designed compounds, may determine the ability to yield a preferred handedness in the product of an asymmetric reaction. In a first investigation, the ability of compound **4** (**Figure 4**) – consisting of a molecular rotary motor functionalized with 4-dimethylaminopyridine and thiourea units – to catalyze the asymmetric Michael addition of 2-methoxythiophenol to 2-cyclohexen-1-one was assessed.[51] As illustrated in **Figure 5**, in the *E*-isomer the functional substituents that can coordinate the substrates are far apart; as a result, this form has a low catalytic activity and leads to a racemic product. Photoisomerization to the *Z*-isomer brings the two substituents close enough to act cooperatively, causing a significant enhancement of the reaction rate and enantioselectivity. The configuration of the product is determined by the relative helical orientation of the aminopyridine and thiourea moieties, which on its turn depends on the helicity of the motor. Thus, the photogenerated unstable (*M,M*)-(*Z*)-isomer affords product in the *S*-configuration; the other enantiomer is obtained upon successive thermal relaxation to the stable (*P,P*)-(*Z*)-form (Figure 5). The last two isomerization steps of the full rotary cycle bring the catalyst back to its initial state. In summary, **4** is a light-driven molecular switch that behaves as a photochemically and thermally responsive catalyst capable of directing the formation of the racemate or either one of the enantiomers of the product in a defined sequence.

<FIGURE 4>

<FIGURE 5>

In a subsequent study,[52] the phenyl spacers that connect the motor to the catalytically active arms in compound **4** were removed in order to enable them to come in greater proximity. It was postulated that if a more constrained pocket could be formed, then an enhanced activity and stereoselectivity may be obtained. This hypothesis was experimentally validated by using the new catalyst in the Henry reaction between nitromethane and trifluoroketones. Along the same line, a chiral bisphosphine species that could function as a ligand for transition metal catalysis was constructed by functionalizing a phosphine moiety to each half of the motor (compound **5** in Figure 4).[53] The activity of the motor-bisphosphine species **5** was investigated in the palladium-catalyzed desymmetrization of *meso*-cyclopent-2-en-1,4-diol bis(carbamate), a well-known test reaction for the enantioselectivity of chiral ligands. When the (*P,P*)-(*E*)-isomer was used as the ligand for Pd, a nearly racemic oxazolidinone product (enantiomeric ratio 53:47) was afforded with 65% yield. Photochemical isomerization yielded the (*M,M*)-(*Z*)-form of **5**, whose palladium complex catalyzes the reaction with a yield of 90% and an enantiomeric ratio of 93:7 in favor of the (*3R,4S*) product. In contrast, after isomerization to the (*P,P*)-(*Z*)-form, the opposite enantiomer (*3S,4R*) was obtained with 85% yield and 6:94 enantiomeric ratio. The switching *in situ* of the palladium catalyst, however, was not possible because of the poor stability of the species generated by UV irradiation and heating.

More recently, compound **6** (**Figure 6**) was obtained by integrating a photoactive molecular rotary motor with a 2,2′-biphenol moiety, which can act as a bidentate ligand for a metal center and form complexes with potential catalytic properties.[54] Owing to the tight steric

coupling of the motor and biphenol moieties, it was hypothesized that the preferred axial chirality of the biaryl (highlighted in green in Figure 6) could be determined by the helicity of the overcrowded alkene core (blue), which in its turn is dictated by the configuration of the stereogenic carbon atom (red). The photoswitching properties of **6**, and the related stereochemical changes, were analyzed in detail by NMR, UV and circular dichroism spectroscopic experiments. Briefly, photochemical excitation causes the reversible switching between the (*R,P,S*$_a$) and (*R,M,R*$_a$) stereoisomers, indicating that a change in the helicity of the motor affects the configuration of the biphenol. The catalytic properties of **6** were examined in an asymmetric addition reaction of diethylzinc to aromatic aldehydes. The active catalyst is formed upon coordination of the biphenol ligand of **6** to a zinc ion. Interestingly, reversal of enantioselectivity upon light irradiation was observed for several substrates, indicating that as far as the chiral induction is concerned the metastable isomer (*R,M,R*$_a$) of the catalyst resembles the enantiomer of the stable isomer (*R,P,S*$_a$). This study demonstrates that switchable chiral catalysts can be obtained by the designed integration of functional elements with well-defined stereochemical properties. The tight conformational coupling that enables the transmission of chiral information from the motor to the catalyst reminds the operation of a mechanical gear (see section 6).

<FIGURE 6>

It is worth noting that the examples described above, as well as other systems presented in the next sections, do not exploit the photoinduced directional, repetitive and autonomous rotary movement characteristic of the motor. As a matter of fact, the overcrowded alkene moiety is used as a simple light-responsive mechanical switch.[55,56] Molecular rotary motors, however, offer a higher degree of control with respect to conventional bistable photochromic

compounds, because they act as multistate switches in which the various states exhibit different structures (e.g. size, shape, helicity) and features (e.g. polarity, optical properties).

4. Affecting cell membranes

An interesting prospective application of synthetic molecular machines is the control of the functions of a cell by means of stimuli-induced changes in its structural features, arising from molecular movements. For example, the disruption of external or internal cellular membranes may be exploited to introduce species into cells, or to promote cell death. To this aim, appropriately functionalized molecular rotary motors of the overcrowded alkene type (section 2.1) were embedded on either synthetic lipid bilayers or cell membranes, and the effect of photochemical irradiation on the membrane stability was investigated.[57] The motors **(Figure 7**) bear either dye moieties (cyanine for **7**, boron dipyrromethene, BODIPY, for **8**) or oligopeptide chains (**9**–**10**) on the lower half; the presence of the dyes does not suppress the photoreactivity of the motor core. Molecular motors with smaller substituents were also considered, as well as a number of control compounds.

<FIGURE 7>

In a first series of experiments, compound **7** and a BODIPY dye were co-entrapped into large unilamellar vesicles (LUVs) self-assembled from phospholipids. Confocal fluorescence microscopy experiments revealed that the BODIPY-based luminescence intensity decreases upon irradiation of the LUV suspension at 365 nm. Control experiments indicated that such a decrease can be attributed to the destabilization of the membrane caused by the photoactivated motion of **7** within the bilayer, thus enabling the escape of the dye. This kind of phenomenon

is interesting but not unprecedented for molecular photoswitches;[58] moreover, the membrane perturbation could not be clearly related to the unidirectional rotation of the motor.

Motors **7** and **8** were later introduced into living cells, and their behavior with and without UV irradiation was studied *in vitro* by optical microscopy.[57] According to the observations, the cell internalization of these compounds is significantly accelerated if they are irradiated with light capable of causing their rotation. The addition of peptide substituents to the molecular motors, as in **9** and **10**, allowed the targeting of specific cells. Little or no cell death was observed upon UV irradiation in control experiments performed with derivatives that are either not photoactive or cannot rotate unidirectionally. This observation indicates that the unidirectional (non-reciprocating) rotation of the molecular motors is crucial to cause their efficient light-induced penetration through the lipid bilayer. The authors hypothesized that membrane rupture and pore formation are induced by a tangential mechanical force exerted by the rotating nanomotors embedded in the bilayer, as sketched in **Figure 8**. Such a mechanism, however, is inconsistent with the facts that, at the molecular level, momentum is largely negligible, and molecular relaxation is likely to be significantly faster than the rotation rate of the motor. Further studies are indeed required to ascertain the origin of these exciting effects. Appropriate functionalization of the motors enables the fluorescence tracking of the molecular motors within cells, or the targeting of specific cell types by exploiting surface recognition elements. All these features offer opportunities for the application of molecular machines to solve biomedical problems.

<FIGURE 8>

5. Transport of molecular cargos

The controlled transfer of substrates within cells is a fundamental function for living organisms. While small molecules and ions can travel efficiently by diffusion, larger objects such as vesicles and organelles would diffuse too slowly across the cytosol, and need to be transported. This task is performed by biomolecular machines such as myosin and kinesin.[2-4] These proteins comprise a motor domain, capable of moving directionally along a track by consuming a fuel (ATP), and a docking domain capable of picking up or releasing appropriate cargos on command. The design and construction of artificial molecular machines that can actively transport molecular or ionic substrates along specific directions, or across membranes, is a fascinating goal for nanoscientists, and may disclose unconventional routes in catalysis, smart materials, energy conversion and storage, and medical therapy.[59,60] Outstanding examples of molecular robots capable of transporting and sorting cargos have been developed by engineering DNA architectures.[61] The development of fully synthetic systems, however, is still at its infancy.

5.1 Linear Molecular Machines

The reversible back-and-forth translation of the ring component along the axle of a rotaxane in controllable molecular shuttles (section 2.2) can be exploited to transport a molecular cargo directionally. As shown schematically in **Figure 9**a, the macrocyclic ring needs to be equipped with a docking site to which the cargo can be attached and detached. From a functional point of view, the following design requirements must be fulfilled: (i) the ring transfer/return and cargo docking/undocking processes have to be independent, reversible, and controlled by non-interfering (orthogonal) stimuli; (ii) the cargo should remain bound to the rotaxane during the movement of the ring. The latter requirement rules out the use of dynamic bonds (e.g., supramolecular interactions) to load the cargo onto the ‘transporter’; kinetically inert, stimuli responsive bonds should be employed.

This device was realized at the proof-of-concept stage with multicomponent rotaxane **11** (Figure 9b), designed to achieve the controlled capture, transport, and release of the metal complex **12** under chemical and photochemical stimulation.[62] The rotaxane consists of a dibenzo[24]crown-8-type ring and a molecular axle containing a dibenzylammonium (A) and a 4,4′-bipyridinium (B) station. In this kind of compounds, the ring encircles selectively the ammonium site. Deprotonation of the latter with a base changes the preferred binding site of the macrocycle, causing its net displacement towards the bipyridinium station; upon regeneration of the ammonium site with an acid, the ring returns on the A station.[63] These movements, which can thus be reversibly controlled by chemical stimulation, occur on the time scale of seconds in solution at room temperature.[64] The macrocycle is endowed with a short chain ending with a nitrile group, that plays the role of anchoring site for the cargo. The latter is a $[Ru(tpy)(bpy)]L^{2+}$ complex in which tpy and bpy are chelating ligands (tpy = 2,2′;6′,2″-terpyridine, bpy = 2,2′-bipyridine) and L is a monodentate ancillary ligand (e.g., an acetonitrile solvent molecule). The behavior of the system was investigated by a combination of ^{1}H NMR and UV-visible spectroscopies, and electrochemical techniques.[62]

<FIGURE 9>

Under appropriate conditions, in an acetone solution containing **12** and an excess of **11** the monodentate ligand of the Ru complex can be replaced by the nitrile terminus of the rotaxane (Figure 9a). This reaction causes the coordination of the cargo to the transporter, whose ring is initially located on the A station. The addition of a base promotes the transfer of the ring towards the bipyridinium station without affecting the cargo, which thus remains attached to the ring. At this stage, irradiation with visible light affords the decoordination of the Ru complex from the nitrile tether of the rotaxane,[65] a process that has no effect on the position

of the ring. Upon addition of an acid, the (unloaded) ring returns at its initial position and in principle the cycle can be repeated; in practice, *in situ* thermal recoordination of **12** to **11** in the dark was not observed, presumably because the vacant coordination position at the ruthenium center gets filled by a ligand (e.g., an anion or an adventitious water molecule) that cannot be displaced by the –CN moiety of **11**.

It should be noted that in the system shown in Figure 9 the transport is ultimately unproductive, because the cargo is picked up and released in the same homogeneous solution. Recent experiments, however, show that appropriately designed rotaxanes embedded in membranes can 'ferry' cargos across physically separated compartments down a concentration gradient.[66] The construction of molecular shuttles capable of using light to transport substrates against a concentration gradient is a fascinating goal that could open up radically new routes in the chemical conversion of solar energy.[67]

5.2 Rotary Molecular Machines

Artificial molecular machines that perform rotary motion have been employed to transfer a cargo intramolecularly between two distinct sites at the extremities of a molecular platform. In such prototypical devices, the molecular rotary switch activates a robotic 'arm' in such a way that its distance from the different extremities of the platform can be changed in response to external stimuli. Another orthogonal stimulus is employed to control the attachment of the cargo at the robotic arm and at either site on the platform, thereby enabling the controlled transfer in either direction. In such a device, and in contrast with the design illustrated in Figure 9a (section 5.1), the cargo is not disconnected from the transporter in any step of the operation mechanism, thus preventing the exchange with other molecules in solution.

A system of this kind, shown in **Figure 10**, is capable of transferring an acetyl group between distant sites within the molecule under the action of light.[68] The activated transporter **13** is an

overcrowded alkene rotary motor endowed with three distinct moieties: a) a phenoxy 'departure site' on one side of the lower half, to which the cargo is initially bound; b) a benzylamine 'arrival site' on the other extremity of the lower half, where the cargo may be delivered after rotation, and; c) a thiol-terminated arm in the upper half that can grasp the cargo. The sequence (Figure 10) starts with the acid-catalyzed cleavage of the trityl and Boc groups that protect respectively the thiol and amine moieties in precursor **14**, followed by treatment with a base. The arm in the upper half picks up the cargo via the reaction of its thiolate moiety with the phenolic ester, yielding a thioacetate. Upon irradiation at 312 nm, rotation around the C=C axis takes place, bringing the thioacetate close to the benzylamine site; acetyl transfer to the amine then occurs, transferring the cargo from the arm to the lower half. The net result of this series of reactions is the intramolecular transport of the acetyl cargo from one extremity of this rigid molecule to the other, covering a distance of about 2 nm.

<FIGURE 10>

6. Transfer of directed motion along molecular components

In a typical machine at the macroscopic scale, a motor – that is, a device that uses an energy source to generate forces – is mechanically coupled to passive elements, such as gears, belts and joints, that are tasked with transmitting and processing the movement. It is true in biological systems too, that the mechanical coupling of molecular motors with other nearby nanoscale components is essential for performing functions.[2-4]

It has been known for decades that synthetic molecules consisting of sterically coupled subunits can exhibit concerted movements.[1,69] Research on this subject has led to the development of molecular species that mimic, at the nanometer scale, the operation of cogwheels,[69,70] bevel gears[71,72] and drive chains.[73] However, as the movement in these

systems is Brownian and hence it lacks directionality, it cannot be used to execute stimuli-induced functions.[74]

6.1 Transmission of rotary movements

An example of synchronous transmission of a photoactivated unidirectional rotary motion from an overcrowded alkene motor to a coupled rotor was reported recently.[75] In compound **15** (**Figure 11**), consisting of a naphthyl rotor covalently appended to the indanyl half of the rotary motor, it was envisioned that the rotation of the naphthyl unit could be locked with the light-triggered motion of the motor. Indeed, NMR and circular dichroism (CD) spectroscopic experiments showed that the naphthyl paddle slides along and rotates around the fluorenyl half of the motor as the latter rotates under the action of light and heat (section 2.1). Interestingly, the naphthyl paddle faces the fluorenyl moiety always with the same side (Figure 11), similarly to what happens for the tidally locked movement of the Moon around the Earth. The precision in the transmission of the motion relies on a fine balance of the steric interactions between the various moving parts: if the fit is too loose, then the coupling is inefficient; if it is too tight, the device is blocked. In the example illustrated in Figure 11, an appropriate balance of the energy barriers associated with the different rotary movements was obtained by a clever molecular design.

<FIGURE 11>

An alternative approach for the intramolecular transmission of unidirectional rotary motion was recently devised and implemented using a light-driven molecular rotary motor of the hemithioindigo family.[76] The operation mechanism of this kind of motors is similar to that of

overcrowded alkenes (Figure 1).[31] In the macrocyclic species **16** (**Figure 12**) the passive rotor is a biaryl unit directly linked to the lower half of the motor, and connected to the upper half by means of an ethylene glycol chain; note that the aryl paddle of the rotor is functionalized off-axis with respect to the rotation axis of the rotor itself. It was anticipated that the photochemically driven unidirectional rotation of the motor could be transmitted to the remote biaryl unit by exploiting the steric strain of the different stereoisomers populated along the operation sequence of the device. NMR and CD spectroscopies, quantum chemical calculations and crystallographic analyses were employed to study the behavior of **16**.

<FIGURE 12>

Such a compound contains three stereogenic elements, namely: (i) point chirality around the sulfoxide unit, (ii) helicity around the motor double bond, and (iii) axial chirality around the biaryl axis. The initial state of the device is the ensemble of the (*R,M,S*$_a$/*R*$_a$)-(*E*) stereoisomers, in which the flexible ethylene glycol chain allows the interconversion between the *R*$_a$ and *S*$_a$ rotamers in dichloromethane solution at room temperature (Figure 12). Upon irradiation at 470 nm the (*R,M,R*$_a$)-(*Z*) isomer is generated; its CD spectrum is indeed consistent with the presence of the biaryl unit in the *R*$_a$ configuration. Indirect evidence and computational modeling suggest that this transformation occurs through the formation of the unstable (*R,P,S*$_a$)-(*Z*) intermediate, which could not be observed experimentally. Subsequent irradiation of the (*R,M,R*$_a$)-(*Z*) form with light of 470 nm affords the (*R,P,R*$_a$)-(*E*) form, which then undergoes thermal relaxation to the initial state. It can thus be concluded that in **16** the light-driven unidirectional rotation of the hemithioindigo moiety is transferred to the passive biaryl rotor owing to the spatially restricted rotational freedom of the latter that arises from the covalent constraints (Figure 12).

It is worth noting that in the systems described in this section the rotation of the motor is autonomous and unidirectional, and such extremely valuable properties are preserved upon transmission.[74] This is a significant step forward in comparison with earlier studies[77] describing the transfer of controlled movements within artificial molecular machines.

6.2 Conversion of rotary motion into linear motion

Coupling rotary and translational movements at the molecular level involves the construction of systems that combine rotary switches or motors, such as those described in section 2.1, with linear machines like rotaxane-based molecular shuttles (section 2.2). A first step along this direction is represented by compound **17**, consisting of a [1]rotaxane in which the (threaded) axle and ring components are linked by means of an overcrowded alkene unit (**Figure 13**).[78] The latter moiety can undergo *E*-*Z* photoisomerization but full unidirectional rotation is not possible. The experimental results demonstrate that the configurational change of the two aromatic halves of the switch, caused by their relative rotation, brings about the linear movement of the pillararene ring along the axle. Although this system contains no molecular motors (both movements are reciprocating), it represents an interesting example of combination of rotary and linear mechanical devices.

<FIGURE 13>

Following a similar design, an overcrowded alkene rotary motor was recently combined with a rotaxane-based molecular shuttle architecture in compound **18** (**Figure 14**a).[79] In this species the upper and lower halves of the molecular motor are functionalized respectively with a crown ether ring and an ammonium-containing axle, which are interlocked together

into a [1]rotaxane architecture. As shown schematically in Figure 14, the deprotonation of the ammonium center of **18** with a base 'unlocks' the crown ether from the axle, and the methyltriazolium (MT) site can go inside the cavity of the ring. Upon UV irradiation the motor begins its rotation cycle, pulling the axle away from the ring (Figure 14b); as a consequence, the latter dissociates from the MT unit and slides along the hydrocarbon chain. The thermal helix inversion of the motor generates the stable *E* form, and the subsequent absorption of another UV photon causes the second half-turn of the motor, pushing the MT unit of the axle back towards the ring. A final helix inversion affords the stable *Z* isomer of the motor, thus completing the cycle. It should be noted that in **18** a unidirectional rotation is transformed into a reciprocating shuttling motion, thus losing directional information. Nevertheless, this study shows that the molecular rotary motor can operate against the non-covalent interactions that would keep the ring around the methyltriazolium site.

<FIGURE 14>

7. Collective effects and macroscopic actuation

Skeletal muscles are able to generate macroscopic forces by accumulating in space and time the forces exerted by a huge number of biomolecular machines, each one generating a force in the order of 10^{-12} N.[2] The basic functional element of the muscle is a μm-sized assembly called sarcomere, that contains the biomolecular motor components (myosin and actin) arranged in interdigitated filaments. Upon gliding of these filaments with respect to one another, triggered by Ca^{2+} ions and fueled by ATP, the sarcomere undergoes a contraction. This transformation is reversible and the sarcomere can recover its original length once the contraction step is over. Hence, the sarcomere shifts the motion from the nanometer to the micrometer scale by collecting the action of several thousands of molecular machines. To

scale up the effect further, thousands of sarcomeres are connected in series to yield myofibrils, which in turn bundle together forming fascicles and thicker fibers. The key for the operation of biological muscles is therefore an amplification of mechanical effects from the nanometer to the macroscopic world by means of a well-defined hierarchical organization that begins at the molecular scale and involves increasingly larger and complex structures.[2-4]

In an artificial context, proof-of-principle experiments performed in the past two decades have shown that the movement of molecular machines can be scaled up to the microscopic[80,81] and macroscopic[82] scales. These attempts involve the deposition of molecular machines on surfaces,[25,26,44,83,84,85,86,87] incorporation in membranes and interfaces,[27,28,88] and integration with crystalline[29,89,90] or polymeric[44,45,91,92] structures. In the next sections investigations aimed at collecting the action of light-powered synthetic molecular machines in organized assemblies, in order to achieve effects at larger length scales, will be illustrated.

7.1 Modified surfaces

The stimuli-induced structural and electronic changes of switchable molecular species deposited on a surface can be exploited to modulate macroscopic properties of the surface itself, such as wettability.[93] This strategy, which has been extensively implemented with photochromic compounds,[83,94] can be applied to molecular machines with the purpose of collecting and amplifying mechanical effects.

In a pioneering study it was shown that light excitation of a rotaxane-based molecular shuttle adsorbed on an appropriately modified metal surface causes the displacement of a liquid droplet across the surface.[95] Rotaxane (*E*)-**19** (**Figure 15**a) consists of a tetralactam macrocycle threaded by an axle that comprises a photoactive fumaramide station and a tetrafluorosuccinamide station. The affinity of the macrocycle for the fumaramide site, arising from hydrogen bonding interactions, is larger than that for the fluorinated succinamide unit;

thus, in the thermodynamically stable form of the rotaxane (*E*), the preferred station for the ring is the fumaramide one. Upon UV light excitation, however, the primary station undergoes $E \rightarrow Z$ isomerization forming the maleamide isomer, which is a very poor recognition site for the ring. As a result, the preferred position for the latter becomes the tetrafluorosuccinamide site. The thermally activated $Z \rightarrow E$ back isomerization regenerates the starting structure, thus completing the shuttling cycle (Figure 15a). It should be noted that the stimuli-induced motion of the ring in **19** has the consequence of concealing or exposing the fluorinated moiety of the axle with respect to the environment. As the wettability of surfaces by polar or apolar liquids is highly sensitive to the presence of fluoroalkane groups on the surface, it was envisioned that the photoinduced shuttling process shown in Figure 15a could be exploited to change the contact angle of a liquid droplet placed on the surface.

<FIGURE 15>

The rotaxane was thus hydrogen-bonded on a monolayer of 11-mercaptoundecanoic acid self-assembled on a glass-supported Au(111) surface (Figure 15b). Indeed, the contact angle measured for small (0.5−5 μL) drops of low-volatility liquids (such as water, formamide, ethylene glycol and diiodomethane) decreased significantly upon irradiation of the surface with ultraviolet light. Control experiments confirmed that the light-induced lowering of the contact angle is related to a reduction in the number of fluoroalkane residues exposed at the surface of the substrate (Figure 15b). Such a photoinduced dewetting was exploited to move the droplets across the surface: when the area ahead of the droplet is irradiated, the liquid is attracted to the switched zone. The collective action of a monolayer of these molecular shuttles is powerful enough to move a droplet of diiodomethane for about one millimeter up to a 12° incline (Figure 15c). This effect is mediated by a change in a bulk physical property;

as such, it is not the result of a direct amplification of motion from the nanometer up to the macroscopic scale. The work, however, is fascinating because a millimeter-size movement is ultimately a consequence of molecular rearrangements in an organized assembly of molecular machines. From an applicative perspective, the transport of liquids using photoresponsive surfaces may prove useful for delivering analytes in lab-on-a-chip setup, or for performing chemical reactions on a tiny scale without reaction vessels, simply by bringing individual drops containing different reactants together.

7.2 Doped liquid crystals

An effective way to transfer structural information from individual molecules to extended supramolecular assemblies is to rely on liquid crystal (LC) phases. Molecular rotary motors such as **20** (**Figure 16**a) can induce the formation of a cholesteric phase when used as enantiopure dopants in nematic LCs.[28,96,97] As the helicity of the motor units determine the pitch of the cholesteric helix, and each step in the rotary process of the molecular motor is accompanied by a change in its helicity, the irradiation of the dopant in the sample brings about a reorganization of the liquid crystal. The photoinduced rearrangement of a thin film of this LC lying atop a polyimide surface caused a rotation of the typical 'fingerprint' cholesteric texture, which could be visualized with the aid of a micrometer-sized glass rod placed on the surface and imaged with an optical microscope (Figure 16b). Upon irradiation at 365 nm light, the rod rotated unidirectionally for a few minutes, until the motion gradually stopped when a photostationary distribution of the motor isomers was reached. Upon turning off the irradiation, reverse rotation of the rod took place until the initial (dark) distribution of the isomers was restored. As expected, if the other enantiomer of the motor is used as the dopant, the rod rotates in the opposite direction. It should be pointed out, however, that the rotation of the rod is not the result of the unidirectional rotation of the molecular motor molecules, but

rather a consequence of the photoinduced change in the distribution of isomers endowed with different helicities. Nevertheless, the exploitation of molecular movements to move a macroscopic object that can be seen to rotate was a landmark accomplishment in the field of molecular machines.

<FIGURE 16>

Another interesting aspect of cholesteric liquid crystals is the fact that droplets of these materials exhibit peculiar topological features, such as microcavities, whose properties are determined by the ratio between the cholesteric pitch and the droplet radius. The photoresponsive behavior of cholesteric LC droplets doped with overcrowded alkene molecular motors was the subject of a recent investigation.[98] Experiments and simulations revealed that the light-induced change of the cholesteric pitch, driven by the switching of the helicity of the molecular motor dopant, can be harnessed to control some properties of the droplet, such as the position of topological defects and the handedness of the radial spherical structure. These results are thought to be of interest for optoelectronic applications that involve the processing of polarized light.[99]

In all the examples described above, the rearrangement of the liquid crystal caused by light irradiation stops as soon as the concentration of the various isomeric forms of the molecular machine reaches a stationary state. A way to circumvent this limitation and maintain the system in a dynamic regime is to modulate the illumination conditions in time and space at the macroscopic scale to obtain an oscillating behavior.[100,101] A LC-based system was recently reported in which the emergence of oscillations under photostationary conditions is the result of a molecular-scale behavior.[102] The liquid crystal, co-doped with an overcrowded alkene molecular rotary motor (e.g. **20** in Figure 16a) and a photo-inactive shape-persistent

1,1′-bi-2-naphthol derivative, was confined between two glass slides spaced by a gap smaller than the pitch of the cholesteric helix. Polarized optical microscopy observations revealed the formation of axially symmetric chiral patterns at low irradiation power (**Figure 17**a). Above a certain irradiation power, a structural symmetry breaking took place spontaneously, leading to non-axisymmetric patterns that feature a kink (Figure 17b). The patterns were seen to rotate continuously under illumination, with both handedness and direction of rotation dictated by the axisymmetric pattern from which they arise. The unidirectional rotation was explained on the basis of the interplay between the twist of the supramolecular LC arrangement and the diffusion of the chiral molecular motors away from a localized illumination area. It was also observed that a particle-like LC structure, trapped in the periphery of the revolving pattern, orbits around the center of the latter; in other words, the light-powered rotation of the LC can be harnessed to move a cargo. In general, it is worth pointing out that this assembly can use the energy of light to establish and maintain non-equilibrium conditions at length scales that are typically four orders of magnitude larger than their molecular components.

<FIGURE 17>

7.3 Self-assembled systems

Supramolecular association phenomena such as gelation and amphiphilic self-assembly can be harnessed to gain control over the orientation and mutual alignment of molecules, with the purpose of developing cooperative effects. For example, photochromic switches have been used to exert photocontrol on solvent gelation[103] and molecular aggregation.[27,104] Systems of this kind are of interest for advanced drug release platforms or for controlling biological processes.

In a recent study, molecular rotary motors of the overcrowded alkene type, rendered amphiphilic by appropriate functionalization, were shown to undergo hierarchical self-organization in aqueous solution (**Figure 18**a).[105,106] In compound **21** (Figure 18b) the motor core bears a dodecyl chain at the upper half, and two carboxyl-terminated alkyl chains at the lower half. The initial stage of the self-assembly of **21** in aqueous NaOH at a concentration of 5% w/w yields micrometer-long fibers with a diameter of about 5-6 nm (Figure 18a). Spectroscopic experiments show that the photoinduced motor function of **21** is preserved in the nanofibers.

<FIGURE 18>

A noodle-like string of centimeter length was then obtained by manually drawing the nanofiber solution into a concentrated aqueous solution of calcium chloride. The shear flow and the electrostatic screening of the Ca^{2+} ions promote the alignment of the nanofibers in the bundles that constitute the string (Figure 18a). If the string is irradiated at 365 nm in water, it readily bends towards the light source (Figure 18c), and it returns to the starting state in 3 hours at 50 °C. The same process could be carried out in air on a suspended string, and a piece of paper of 0.4 mg adhered to its end could be lifted. The photoactuation mechanism was investigated by *in situ* small-angle X-ray scattering (SAXS) experiments. Presumably, the photoinduced transformation of the motor from the stable to the unstable isomer elicits an increase of the excluded volume around the motor, which in turn causes a perturbation of the local packing arrangement, with the overall effect of thickening and shortening the fibers. Because of the thickness of the string (~300 μm) and its optical density at the irradiation wavelength (due to the absorbance of the motor), the contraction can only take place at the irradiated side of the string, which thus bends towards the light source.[105] It is worth noting

that, once again, unidirectional motion is not actually important to the function of the system. Nevertheless, the fact that a material self-assembled in ambient conditions and consisting of 95% water can do macroscopic work, accomplished by collecting and amplifying molecular movements, is very remarkable, and augurs well for the fabrication of low cost, biocompatible molecular-machine-based soft actuators.

7.4 Polymers

Another promising strategy for scaling up motion from the nanometer to the macroscopic scale appears to be the integration of molecular machines into polymers.[44,45,84,91,92] An effective design involves the head-to-tail connection of [c2]daisy chain doubly interlocked rotaxane species that can expand and contract in response to external stimuli (section 2.2). From a functional viewpoint, this design mimics the amplification mechanism that takes place in myofibrils of skeletal muscles (see section 7). In the past few years, chemically switchable [c2]daisy chains have been employed to construct coordination[81] or supramolecular[107] polymers wherein molecular movements are transferred to the microscopic domain. Furthermore, co-polymerization of suitably functionalized [c2]daisy chain monomers with linear and branched connectors has led to the preparation of crosslinked covalent polymers.[82] In these materials, the synchronous collective mechanical switching between contracted and expanded forms of the monomers, triggered by pH variations, can produce a macroscopic size change.

Light-activated [c2]daisy chain species, with a design similar to that of compound **3** (Figure 3), were recently incorporated in polymer networks to construct photoresponsive wet- and dry-type gels.[108] The polymer (**Figure 19**a) was obtained by the polycondensation of α-cyclodextrin-azobenzene [c2]daisy chain rotaxanes[48] and tetra(polyethylene glycol) connectors, and was employed to prepare hydrogels and xerogels.[109] It was found that

irradiation with UV light reduces the volume of a square-shaped hydrogel fragment, while exposure to visible light restores its initial size (Figure 19b). This behavior was related to the UV light-induced contraction and visible light-induced extension of the daisy chains arising from $E \rightarrow Z$ and $Z \rightarrow E$ isomerization, respectively (Figure 19c). Interestingly, an analogous hydrogel containing only azobenzene as switchable units showed an opposite behavior; in that case, the distance between the crosslinking points increases upon $E \rightarrow Z$ photoisomerization. In fact, the two hydrogels contract and expand according to different mechanisms. In the azobenzene gel the transition from the hydrophobic *E*-form to the more polar *Z*-isomer causes a decrease in crosslinking density, with consequent release of water. Conversely, in the daisy chain-based gel the swelling and deswelling is controlled by the change in the end-to-end distance of the molecular machine units (Figure 19c).

<FIGURE 19>

The photoinduced motion could be better evidenced by irradiating a stripe of gel suspended in water (Figure 19d). Illumination from a side resulted in the bending of the strip towards the light source. As discussed in section 7.3, this phenomenon is due to the fact that, because of the partial penetration of the light, only the molecular machines at the irradiated surface can be activated, and not those at the other side. Under the conditions employed, the maximum bending amplitude was reached after 3 hours of exposure to 365-nm light, whereas the recovery by visible light occurred in minutes; the switching cycle could be repeated several times without loss of efficiency or apparent degradation of the material.

A remarkable aspect of this system, and uncommon for polymer-based actuators, is that photoinduced actuation is maintained even if the aqueous solvent is removed from the gel. In fact, a xerogel obtained by freezing and lyophilization of the daisy chain-based hydrogel

(Figure 19), studied under similar conditions, also exhibited bending towards the light source, with a much faster response with respect to the hydrogel (Figure 19d). In this case, however, UV irradiation on the other side of the gel stripe was necessary to recover the initial shape, and a permanent reduction in size was observed after cycling. This pseudo-reversible behavior was attributed to the fact that hydrophobic interactions (which contribute to drive the shuttling of the α-CD macrocycles in the daisy chains) and swelling forces are missing in the xerogel.

In another series of investigations, overcrowded alkene molecular rotary motors were incorporated in polymeric gels and the effect of UV irradiation on the resulting materials was examined.[110,111] Upon functionalization of the upper and lower halves of the enantiopure motor with two azide-terminated poly(ethylene glycol) chains and two alkyne-terminated oligo(ethylene glycol) chains, respectively, compound **22** (**Figure 20**a) was obtained. A crosslinked polymer was then prepared by submitting **22** to Cu-catalyzed alkyne-azide cycloaddition (Cu-AAC) under high concentration conditions, which resulted in the covalent connection of the ethylene glycol chains attached to different motors by means of triazole moieties, as shown in Figure 20a. Such a polymer forms a gel in toluene at 10% w/w, which was studied by SAXS, atomic force microscopy, and DFT calculations. Interestingly, UV irradiation caused the contraction of a millimeter-sized fragment of the gel – a change that could be clearly seen by the naked eye (Figure 20b). It was hypothesized that the entangled polymer chains may become coiled up as a consequence of the light-driven unidirectional rotation of the motor moieties, as schematically depicted in Figure 20c. Such an interpretation is supported by the results of experiments carried out on figure-of-eight-shaped macromolecules prepared by performing the Cu-AAC reaction on **22** under dilute conditions, in order to join the reactive chains intramolecularly. Individual figure-of-eight-shaped objects imaged by AFM were found to exhibit a transition to a collapsed, more compact shape upon illumination with UV light, a result consistent with the motor-driven formation of a wound structure.

<FIGURE 20>

It should be pointed out that this system exploits the unidirectional autonomous movement of a molecular motor powered by a single stationary (that is, non-modulated) optical stimulus. As such, it is substantially different from materials, like the one described in Figure 19, based on bistable mechanical molecular switches that are reversibly interconverted between two states by different stimuli. In fact, the continuous photoinduced rotation of the motor units in the polymer gel (Figure 20c) drives the system progressively away from thermal equilibrium, and the energy of incident photons is converted into free energy of the entangled polymer chains through reduction in their conformational entropy. Hence, the light energy is stored in the gel (the estimated conversion efficiency is 0.15%), but it cannot be retrieved because the braiding of the polymer chains is irreversible. This issue was addressed in a later work[112] by introducing photoswitchable units in the crosslinked network that could function as 'modulator' elements on demand, that is, to release the elastic potential energy by unbraiding the polymer chains. To this aim, compound **23** (similar to **22** but containing only alkyne ends) was co-polymerized with the azide-terminated diarylethene derivative **24** (**Figure 21**a) to yield a polymeric gel embedding both modulator and motor subunits and analogous to that described in Figure 20.

A key feature of this design is that the modulator units can be operated at a different wavelength than that used to activate the rotary motors. Specifically, UV irradiation powers the unidirectional rotation of the motors (Figure 20c) but it does not affect the diarylethene units which thus remain in their closed (locked) form (Figure 21b), thereby promoting the braiding of the polymer chains caused by the motors. In contrast, irradiation with visible light converts the modulators into their open (unlocked) form (Figure 21b), while it is ineffective

for the activation of the motors. Thanks to the elastic behavior of the polymer, the torsional energy stored in the coiled chains can be released by free rotation around the C–C single bonds of the diarylethene units, until thermodynamic equilibrium is reached.

It is interesting to note that if the material is irradiated simultaneously with UV and visible light, the motors wind the polymer chains and the modulators tend to unwind them (Figure 21c). Hence, upon regulating the relative intensities of UV and visible light, the braiding and unbraiding rates can be tuned, ultimately determining whether the gel is contracting or expanding; if such rates are identical, an out-of-equilibrium photostationary state is reached. The energy accumulated in the material and its mechanical output can be adjusted by optically modulating the winding and unwinding frequencies. This study shows that different types of light-activated molecular devices can be functionally incorporated in a polymeric material by precise molecular design, and constitutes a step forward towards the construction of more sophisticated molecular motor-based systems capable of converting light energy into potential and mechanical energy that can be retrieved on demand.

<FIGURE 21>

8. Conclusion

Molecular machinists, since the origins of the field – which can be symbolically dated back to the famous Feynman's talk on nanotechnology[113] – have conformed to two philosophically different design strategies: technomimetic and biomimetic. Indeed, the blueprints of working schemes and building blocks that are well known in the engineering realm could inspire the conception of mechanical machines at the extreme level of miniaturization – that is, at the molecular scale. This approach, which can take advantage of well-established paradigms and a widespread terminology, proved extremely useful to popularize the idea of molecular

machines among the general public and, at earlier stages, also among scientists.[114] On the other hand, it is now widely accepted that molecular machines are not merely shrunken versions of the macroscopic ones and operate by following very different rules.[115] In fact, the biomolecular machines that work marvelously in living organisms highlight the astonishing things that could be done if one could master the complex rules of nature, and justify the huge interest and rapid development of the area of synthetic molecular machines. The two approaches mentioned above are not mutually exclusive and are often combined together, as also demonstrated by the examples described in this review.

One of the most challenging and motivating issues associated with the design of an artificial molecular machine is the function that it may be able to perform. In this regard, inspiration can come both from nature (e.g. enzyme-type systems, transport of substrates, operation in membranes) and technology (catalysis, transmission of motion, materials for mechanical actuation and energy conversion). Having said that, the added value of the machines discussed here is the use of light as an energy source – a fact which is relatively rare for biological systems but highly desirable from a technological viewpoint.

Despite the huge advancements in the field, it must be recognized that synthetic molecular machines are still far from real world applications. Among the relevant issues that should be addressed are expanding the choice of building blocks and assembly architectures, and inventing novel working schemes. As a matter of fact, most examples of application of molecular machines reported until now make use of overcrowded alkenes rotary motors; only a few of them rely on mechanically interlocked molecules. Moreover, the majority of photoactivated functional molecular machines reported to date rely on photochemical reactions, commonly photoisomerization; besides considering novel photochromic compounds, other currently underexploited light-induced processes, such as electron transfer or proton transfer, may be considered. The aspect requiring the strongest research effort,

however, is the integration of molecular machines with their environment such that the molecular motion can produce an effect. The proof-of-principle examples discussed here demonstrate that this objective is nowadays within the reach of scientists, and that the peculiar features of the light-matter interaction can play a prominent role in developing molecular machine-based devices and materials able to make breakthroughs in technology and medicine.

Acknowledgements

Financial support from the Ministero dell'Istruzione, Università e Ricerca (FARE Grant R16S9XXKX3), the University of Bologna and the National Research Council of Italy is gratefully acknowledged.

Received: ((will be filled in by the editorial staff))

Revised: ((will be filled in by the editorial staff))

Published online: ((will be filled in by the editorial staff))

References

[1] V. Balzani, A. Credi, M. Venturi, *Molecular Devices and Machines – Concepts and Perspectives for the Nanoworld*, Wiley-VCH, Weinheim, Germany **2008**.

[2] *Molecular Motors* (Ed.: M. Schliwa), Wiley-VCH, Weinheim, Germany **2003**.

[3] D. S. Goodsell, *Bionanotechnology - Lessons from Nature*, Wiley-Liss, Hoboken, NJ, USA **2004**.

[4] R. A. L. Jones, *Soft Machines - Nanotechnology and Life*, Oxford University Press, Oxford, UK **2008**.

[5] S. Erbas-Cakmak, D. A. Leigh, C. T. McTernan, A. L. Nussbaumer, *Chem. Rev.* **2015**, *115*, 10081.

[6] S. Kassem, T. van Leeuwen, A. S. Lubbe, M. R. Wilson, B. L. Feringa, D. A. Leigh, *Chem. Soc. Rev.* **2017**, *46*, 2592.

[7] C. Pezzato, C. Cheng, J. F. Stoddart, R. D. Astumian, *Chem. Soc. Rev.* **2017**, *46*, 5491.

[8] M. Baroncini, L. Casimiro, C. de Vet, J. Groppi, S. Silvi, A. Credi, *ChemistryOpen* **2018**, *7*, 169.

[9] R. D. Astumian, *Phys. Chem. Chem. Phys.* **2007**, *9*, 5067.

[10] B. L. Feringa, *Angew. Chem. Int. Ed.* **2017**, *56*, 11060.

[11] J.-P. Sauvage, *Angew. Chem. Int. Ed.* **2017**, *56*, 11080.

[12] J. F. Stoddart, *Angew. Chem. Int. Ed.* **2017**, *56*, 11094.

[13] S. Silvi, M. Venturi, A. Credi, *Chem. Commun.* **2011**, *47*, 2483.

[14] J. Groppi, M. Baroncini, S. Silvi, M. Venturi, A. Credi, *Chem. Commun.* **2019**, *55*, 12595.

[15] P. Ceroni, A. Credi, M. Venturi, *Chem. Soc. Rev.* **2014**, *43*, 4068.

[16] M. Katan, S. Hecht, *Chem. Soc. Rev.* **2017**, *46*, 5536.

[17] M. Baroncini, S. Silvi, A. Credi, *Chem. Rev.* **2019**, *119*, DOI: 10.1021/acs.chemrev.9b00291.

[18] *Mechanisms of Primary Energy Transduction in Biology* (Ed.: M. Wikström), RSC Publishing, Cambridge, UK **2018**.

[19] V. Balzani, A. Credi, M. Venturi, *ChemSusChem* **2008**, *1*, 26.

[20] A. Coskun, M. Banaszak, R. D. Astumian, J. F. Stoddart, B. A. Grzybowski, *Chem. Soc. Rev.* **2012**, *41*, 19.

[21] T. van Leeuwen, A. S. Lubbe, P. Štacko, S. J. Wezenberg, B. L. Feringa, *Nat. Rev. Chem.* **2017**, *1*, 0096.

[22] Q. Wang, D. Chen, H. Tian, *Sci. China Chem.* **2018**, *61*, 1261.

[23] N. Koumura, R. W. J. Zijlstra, R. A. van Delden, N. Harada, B. L. Feringa, *Nature* **1999**, *401*, 152.

[24] D. Roke, S. J. Wezenberg, B. L. Feringa, *Proc. Nat. Acad. Sci. U.S.A.* **2018**, *115*, 9423, and references therein.

[25] B. Krajnik, J. Chen, M. A. Watson, S. L. Cockroft, B. L. Feringa, J. Hofkens, *J. Am. Chem. Soc.* **2017**, *139*, 7156.

[26] J. Kaleta, J. Chen, G. Bastien, M. Dračínský, M. Mašát, C. T. Rogers, B. L. Feringa, J. Michl, *J. Am. Chem. Soc.* **2017**, *139*, 10486.

[27] D. J. van Dijken, J. Chen, M. C. A. Stuart, L. Hou, B. L. Feringa, *J. Am. Chem. Soc.* **2016**, *138*, 660.

[28] R. Eelkema, M. M. Pollard, N. Katsonis, J. Vicario, D. J. Broer, B. L. Feringa, *J. Am. Chem. Soc.* **2006**, *128*, 14397.

[29] W. Danowski, T. van Leeuwen, S. Abdolahzadeh, D. Roke, W. R. Browne, S. J. Wezenberg, B. L. Feringa. *Nat. Nanotechnol.* **2019**, *14*, 488.

[30] L. Greb, J.-M. Lehn, *J. Am. Chem. Soc.* **2014**, *136*, 13114.

[31] M. Guentner, M. Schildhauer, S. Thumser, P. Mayer, D. Stephenson, P. J. Mayer, H. Dube, *Nat. Commun.* **2015**, *6*, 8406.

[32] D. A. Leigh, J. K. Y. Wong, F. Dehez, F. Zerbetto, *Nature* **2003**, *424*, 174.

[33] P. L. Anelli, N. Spencer, J. F. Stoddart, *J. Am. Chem. Soc.* **1991**, *113*, 5131.

[34] R. A. Bissell, E. Córdova, A. E. Kaifer, J. F. Stoddart, *Nature* **1994**, *369*, 133.

[35] A. M. Brouwer, C. Frochot, F. G. Gatti, D. A. Leigh, L. Mottier, F. Paolucci, S. Roffia, G. W. H. Wurpel, *Science* **2001**, *291*, 2124.

[36] V. Balzani, M. Clemente-Leon, A. Credi, B. Ferrer, M. Venturi, A. H. Flood, J. F. Stoddart, *Proc. Natl. Acad. Sci. U. S. A.* **2006**, *103*, 1178.

[37] H. Li, A.C. Fahrenbach, A. Coskun, Z. Zhu, G. Barin, Y.-L. Zhao, Y.Y. Botros, J.-P.Sauvage, J.F. Stoddart, *Angew. Chem. Int. Ed.* **2011**, *50*, 6782.

[38] C. A. Stanier, S. J. Alderman, T. D. W. Claridge, H. L. Anderson, *Angew. Chem. Int. Ed.* **2002**, *41*, 1769.

[39] D.-H. Qu, Q.-C. Wang, X. Ma, H. Tian, *Chem. Eur. J.* **2005**, *11*, 5929.

[40] H. Murakami, A. Kawabuchi, R. Matsumoto, T. Ido, N. Nakashima, *J. Am. Chem. Soc.* **2005**, *127*, 15891.

[41] Recent review: S. Yu, N. D. McClenaghan, J.-L. Pozzo, *Photochem. Photobiol. Sci.* **2019**, *18*, 2102.

[42] I. Willner, V. Pardo-Yssar, E. Katz, K. T. Ranjit, *J. Electroanal. Chem.* **2001**, *497*, 172.

[43] M. C. Jiménez, C. Dietrich-Buchecker, J.-P. Sauvage, *Angew. Chem. Int. Ed.* **2000**, *39*, 3284.

[44] C. J. Bruns, J. F. Stoddart, *Acc. Chem. Res.* **2014**, *47*, 2186.

[45] A. Goujon, E. Moulin, G. Fuks, N. Giuseppone, *CCS Chem.* **2019**, *1*, 83.

[46] R. E. Dawson, S. F. Lincoln, C. J. Easton, *Chem. Commun.* **2008**, 3980.

[47] S. Tsuda, Y. Aso, T. Kaneda, *Chem. Commun.* **2006**, 3072.

[48] S. Li, D. Taura, A. Hashidzume, A. Harada, *Chem. Asian J.* **2010**, *5*, 2281.

[49] V. Blanco, D. A. Leigh, V. Marcos, *Chem. Soc. Rev.* **2015**, *44*, 5341.

[50] M. Vlatković, B. S. L. Collins, B. L. Feringa, *Chem. Eur. J.* **2016**, *22*, 17080.

[51] J. Wang, B. L. Feringa, *Science* **2011**, *331*, 1429.

[52] M. Vlatković, L. Bernardi, E. Otten, B. L. Feringa, *Chem. Commun.* **2014**, *50*, 7773.

[53] D. Zhao, T. M. Neubauer, B. L. Feringa, *Nat. Commun.* **2015**, *6*, 6652.

[54] S. F. Pizzolato, P. Štacko, J. C. M. Kistemaker, T. van Leeuwen, E. Otten, B. L. Feringa, *J. Am. Chem. Soc.* **2018**, *140*, 17278.

[55] L. Wang, Q. Li, *Chem. Soc. Rev.* **2018**, *47*, 1044.

[56] Z. L. Pianowski, *Chem. Eur. J.* **2019**, *25*, 5128.

[57] V. García-López, F. Chen, L. G. Nilewski, G. Duret, A. Aliyan, A. B. Kolomeisky, J. T. Robinson, G. Wang, R. Pal, J. M. Tour, *Nature* **2017**, *548*, 567.

[58] D. Wandera, S. R. Wickramasinghe, S. M. Husson, *J. Membr. Sci.* **2010**, *357*, 6.

[59] See, e.g.: R. K. O'Reilly, A. J. Turberfield, T. R. Wilks, *Acc. Chem. Res.* **2017**, *50*, 2496.

[60] See, e.g.: G. De Bo, M. A. Y. Gall, S. Kuschel, J. De Winter, P. Gerbaux, D. A. Leigh, *Nat. Nanotechnol.* **2018**, *13*, 381.

[61] See, e.g.: A. J. Thubagere, W. Li, R. F. Johnson, Z. Chen, S. Doroudi, Y. L. Lee, G. Izatt, S. Wittman, N. Srinivas, D. Woods, E. Winfree, L. Qian, *Science* **2017**, *357*, eaan6558.

[62] C. Schäfer, G. Ragazzon, B. Colasson, M. La Rosa, S. Silvi, A. Credi, *ChemistryOpen* **2016**, *5*, 120.

[63] P. R. Ashton, R. Ballardini, V. Balzani, I. Baxter, A. Credi, M. C. T. Fyfe, M. T. Gandolfi, M. Gómez-López, M. V. Martínez-Díaz, A. Piersanti, N. Spencer, J. F. Stoddart, M. Venturi, A. J. P. White, D. J. Williams, *J. Am. Chem. Soc.* **1998**, *120*, 11932.

[64] S. Garaudée, S. Silvi, M. Venturi, A. Credi, A. H. Flood, J. F. Stoddart, *ChemPhysChem* **2005**, *6*, 2145.

[65] P. Mobian, J.-M. Kern, J.-P. Sauvage, *Angew. Chem. Int. Ed.* **2004**, *43*, 2392.

[66] S. Chen, Y. Wang, T. Nie, C. Bao, C. Wang, T. Xu, Q. Lin, D.-H. Qu, X. Gong, Y. Yang, L. Zhu, H. Tian, *J. Am. Chem. Soc.* **2018**, *140*, 17992.

[67] A. Credi, *Angew. Chem. Int. Ed.* **2019**, *58*, 4108.

[68] J. Chen, S. J. Wezenberg, B. L. Feringa, *Chem. Commun.* **2016**, *52*, 6765.

[69] H. Iwamura, K. Mislow, *Acc. Chem. Res.* **1988**, *21*, 175.

[70] H. Kwart, S. Alekman, *J. Am. Chem. Soc.* **1968**, *90*, 4482.

[71] A. M. Stevens, C. J. Richards, *Tetrahedron Lett.* **1997**, *38*, 7805.

[72] S. Ogi, T. Ikeda, R. Wakabayashi, S. Shinkai, M. Takeuchi, *Chem. Eur. J.* **2010**, *16*, 8285.

[73] S. Liu, D. V. Kondratuk, S. A. L. Rousseaux, G. Gil-Ramírez, M. C. O'Sullivan, J. Cremers, T. D. W. Claridge, H. W. Anderson, *Angew. Chem. Int. Ed.* **2015**, *54*, 5355.

[74] M. Baroncini, A. Credi, *Science* **2017**, *356*, 906.

[75] P. Štacko, J. C. M. Kistemaker, T. van Leeuwen, M.-C. Chang, E. Otten, B. L. Feringa, *Science* **2017**, *356*, 964.

[76] E. Uhl, S. Thumser, P. Mayer, H. Dube, *Angew. Chem. Int. Ed.* **2018**, *57*, 11064.

[77] See, e.g.: T. Muraoka, K. Kinbara, T. Aida, *Nature* **2006**, *440*, 512.

[78] Y. Wang, T. Tian, Y.-Z. Chen, L.-Y. Niu, L.-Z. Wu, C.-H. Tung, Q.-Z. Yang, R. Boulatov, *Chem. Commun.* **2018**, *54*, 7991.

[79] J.-J. Yu, L.-Y. Zhao, Z.-T. Shi, Q. Zhang, G. London, W.-J. Liang, C. Gao, M.-M. Li, X.-M. Cao, H. Tian, B. L. Feringa, D.-H. Qu, *J. Org. Chem.* **2019**, *84*, 5790.

[80] Y. Liu, A. H. Flood, P. A. Bonvallet, S. A. Vignon, B. H. Northrop, H.-R. Tseng, J. O. Jeppesen, T. J. Huang, B. Brough, M. Baller, S. Magonov, S. D. Solares, W. A. Goddard, C.-M. Ho, J. F. Stoddart, *J. Am. Chem. Soc.* **2005**, *127*, 9745.

[81] G. Y. Du, E. Moulin, N. Jouault, E. Buhler, N. Giuseppone, *Angew. Chem. Int. Ed.* **2012**, *51*, 12504.

[82] A. Goujon, T. Lang, G. Mariani, E. Moulin, G. Fuks, J. Raya, E. Buhler, N. Giuseppone, *J. Am. Chem. Soc.* **2017**, *139*, 14825.

[83] N. Katsonis, M. Lubomska, M. M. Pollard, B. L. Feringa, *Progr. Surf. Sci.* **2007**, *82*, 407.

[84] S. Silvi, M. Venturi, A. Credi, *J. Mater. Chem.* **2009**, *19*, 2279.

[85] B. K. Pathem, S. A. Claridge, Y. B. Zheng, P. S. Weiss, *Annu. Rev. Phys. Chem.* **2013**, *64*, 605.

[86] See, e.g.: Q. Zhang, S.-J. Rao, T. Xie, X. Li, T.-Y. Xu, D.-W. Li, D.-H. Qu, Y.-T. Long, H. Tian, *Chem* **2018**, *4*, 2670.

[87] See, e.g.: T. Heinrich, C. H. H. Traulsen, M. Holzweber, S. Richter, V. Kunz, S. K. Kastner, S. O. Krabbenborg, J. Huskens, W. E. S. Unger, C. A. Schalley, *J. Am. Chem. Soc.* **2015**, *137*, 4382.

[88] M. A. Watson, S. L. Cockroft, *Chem. Soc. Rev.* **2016**, *45*, 6118.

[89] See, e.g.: S. Ohshima, M. Morimoto, M. Irie, *Chem. Sci.* **2015**, *6*, 5746.

[90] See, e.g.: M. Baroncini, S. d'Agostino, G. Bergamini, P. Ceroni, A. Comotti, P. Sozzani, I. Bassanetti, F. Grepioni, T. M. Hernandez, S. Silvi, M. Venturi, A. Credi, *Nat. Chem.* **2015**, *7*, 634.

[91] L. Fang, M. A. Olson, D. Benitez, E. Tkatchouk, W. A. Goddard III, J. F. Stoddart, *Chem. Soc. Rev.* **2010**, *39*, 17.

[92] X. Yan, B. Zheng, F. Huang, *Polym. Chem.* **2013**, *4*, 2395.

[93] *Stimuli-responsive dewetting/wetting smart surfaces and interfaces* (Eds: A. Hozumi, L. Jiang, H. Lee, M. Shimomura), Springer, Cham, Switzerland **2018**.

[94] See, e.g.: G. B. Demirel, N. Dilsiz, M. Çakmak, T. Çaykara, *J. Mater. Chem.* **2011**, *21*, 3189.

[95] J. Berna, D. A. Leigh, M. Lubomska, S. M. Mendoza, E. M. Pérez, P. Rudolf, G. Teobaldi, F. Zerbetto, *Nat. Mater.* **2005**, *4*, 704.

[96] R. Eelkema, M. M. Pollard, J. Vicario, N. Katsonis, B. S. Ramon, C. W: M. Bastiaansen, D. J. Broer, B. L. Feringa, *Nature* **2006**, *440*.

[97] A. Bosco, M. G. M. Jongejan, R. Eelkema, N. Katsonis, E. Lacaze, A. Ferrarini, B. L. Feringa, *J. Am. Chem. Soc.* **2008**, *130*, 14615.

[98] P. Sleczkowki, Y. Zhou, S. Iamsaard, J. J. de Pablo, N. Katsonis, E. Lacaze, *Proc. Natl. Acad. Sci. U. S. A.* **2018**, *115*, 4334.

[99] A. Ryabchun, A. Bobrovsky, *Adv. Opt. Mater.* **2018**, *6*, 1800334.

[100] For a recent discussion, see: H. Zeng, P. Wasylczyk, D. S. Wiersma, A. Priimagi, *Adv. Mater.* **2018**, *30*, 1703554.

[101] See, e.g.: A. H. Gelebart, D. J. Mulder, M. Varga, A. Konya, G. Vantomme, E. W. Meijer, R. L. B. Selinger, D. J. Broer, *Nature* **2017**, *546*, 632.

[102] T. Orlova, F. Lancia, C. Loussert, S. Iamsaard, N. Katsonis, E. Brasselet, *Nat. Nanotechnol.* **2018**, *13*, 304.

[103] See, e.g.: S. J. Wezenberg, C. M. Croisetu, C. M. A. Stuart, B. L. Feringa, *Chem. Sci.* **2016**, *7*, 4341.

[104] See, e.g.: J.-J. Yu, Z.-Q. Cao, Q. Zhang, S. Yang, D.-H. Qu, H. Tian, *Chem. Commun.* **2016**, *52*, 12056.

[105] J. Chen, F. K.-C. Leung, M. C. A. Stuart, T. Kajitani, T. Fukushima, E. van der Giessen, B. L. Feringa, *Nat. Chem.* **2018**, *10*, 132.

[106] F. K.-C. Leung, T. van den Enk, T. Kajitani, J. Chen, M. C. A. Stuart, J. Kuipers, T. Fukushima, B. L. Feringa, *J. Am. Chem. Soc.* **2018**, *140*, 17724.

[107] A. Goujon, G. Du, E. Moulin, G. Fuks, M. Maaloum, E. Buhler, N. Giuseppone, *Angew. Chem. Int. Ed.* **2016**, *55*, 703.

[108] K. Iwaso, Y. Takashima, A. Harada, *Nat. Chem.* **2016**, *8*, 626.

[109] For a related example, see: Y. Takashima, S. Hatanaka, M. Otsubo, M. Nakahata, T. Kakuta, A. Hashidzume, H. Yamaguchi, A. Harada, *Nat. Commun.* **2012**, *3*, 1270.

[110] Q. Li, G. Fuks, E. Moulin, M. Maaloum, M. Rawiso, I. Kulic, J. T. Foy, N. Giuseppone, *Nat. Nanotechnol.* **2015**, *10*, 161.

[111] J.-R. Colard-Itté, Q. Li, D. Collin, G. Mariani, G. Fuks, E. Moulin, E. Buhler, N. Giuseppone, *Nanoscale* **2019**, *11*, 5197.

[112] J. T. Foy, Q. Li, A. Goujon, J.-R. Colard-Itté, G. Fuks, E. Moulin, O. Schiffmann, D. Dattler, D. P. Funeriu, N. Giuseppone, *Nat. Nanotechnol.* **2017**, *12*, 540.

[113] R. P. Feynman, *Eng. Sci.* **1960**, *23*, 22.

[114] V. Balzani, A. Credi, F. M. Raymo, J. F. Stoddart, *Angew. Chem. Int. Ed.* **2000**, *39*, 3348.

[115] L. Zhang, V. Marcos, D. A. Leigh *Proc. Natl. Acad. Sci. U. S. A.* **2018**, *115*, 9397.

Figure captions

Figure 1. (a) Scheme of the photochemically activated unidirectional 360° rotation in molecular rotary motor **1**.[23] The starting point of the cycle is the upper left isomer. (b) Simplified potential energy profile showing the alternated light driven energetically uphill and the thermally driven downhill steps. Adapted with permission.[6] Copyright 2017 The Royal Society of Chemistry.

Figure 2. Light-induced ring shuttling in the surface-bound rotaxane **2** controlled by the reversible *E*-*Z* isomerization of azobenzene.[42] The molecular rings are β-cyclodextrin units.

Figure 3. Photochemical switching between extended and contracted structures in the stilbene-containing rotaxane dimer **3**.[46] The molecular rings are α-cyclodextrin units.

Figure 4. Structure formula of the molecular motor-catalyst conjugates **4**[51] and **5**[53] in their (*P,P*)-(*E*) form.

Figure 5. The effect of the light- and thermally-driven switching of **4** on the stereochemistry of the product of the Michael addition between 2-methoxythiophenol and 2-cyclohexen-1-one. Adapted with permission.[21] Copyright 2017 Springer Nature.

Figure 6. Design, structural formula, and photoinduced switching of the motor-catalyst conjugate **6**. This compound features point-to-helical-to-axial-to-point transfer of chirality, a

property manifested in its catalytic activity in an enantioselective addition. Reproduced with permission.[54] Copyright 2018 American Chemical Society.

Figure 7. Structure formulas of molecular rotary motors **7**–**10**, employed to investigate the photo-destabilization of bilayer membranes.[57]

Figure 8. Schematic representation of molecular motors physisorbed on a cell membrane, and of their UV-induced rotation inducing membrane disruption and pore formation. Reproduced with permission.[57] Copyright 2017 Springer Nature.

Figure 9. (a) Design of a 'molecular transporter' based on a controllable molecular shuttle and operated by two independent external stimuli (base/acid and dark/light). (b) Structure formulas of the rotaxane transporter **11** and cargo **12**.[62]

Figure 10. Structure formulas of the molecular device **13** and its protected precursor **14**, based on a molecular rotary motor, and operation scheme for the chemically and photochemically triggered transport of an acetyl cargo (red) from a phenoxy 'departure' site (blue) to a benzylamine 'arrival' site (green).[68]

Figure 11. Operation cycle showing the transfer of a directionally controlled rotary movement from the motor to the rotor component in compound **15**.[75] The starting point of the cycle is the upper left structure. Unidirectional rotation of the overcrowded alkene moieties (blue and grey) makes the appended naphthyl paddle (red) revolve around the motor axis and rotate around the rotor axis, facing the fluorenyl moiety always with the same side.

Adapted with permission.[74] Copyright 2017 American Association for the Advancement of Science.

Figure 12. The photochemically and thermally driven steps at the basis of the transmission of unidirectional rotation from the hemithioindigo motor (blue and grey) to an aryl unit (red) by means of a flexible ethylene glycol connector in macrocycle **16**.[76]

Figure 13. Schematic representation of the photoinduced switching in [1]rotaxane **17**, wherein the flapping movement of the alkene unit is transformed into the translation of the pillararene macrocycle along the axle.[78]

Figure 14. (a) Structure formula of compound **18** comprising a photochemically driven molecular rotary motor and a [1]rotaxane moiety. The ring is initially kept around the ammonium recognition site and can be 'unlocked' by deprotonation of the ammonium center with a base. (b) Scheme of the light-driven rotation of the motor, resulting in the concomitant translation of the ring with respect to the axle. Adapted with permission.[79] Copyright 2019 American Chemical Society.

Figure 15. (a) Structural formula of rotaxane **19** and its operation as a photocontrolled molecular shuttle. The tetralactam macrocycle (light blue) moves between the fumaramide (green) and tetrafluorosuccinamide (orange) stations. (b) Representation of the light-induced change of the hydrophobic/hydrophilic character of a gold surface covered with a self-assembled monolayer of rotaxane **19** and 11-mercaptoundecanoic acid. As illustrated schematically, at the photostationary state about 50% of the fumaramide units have been

isomerized. (c) Lateral photographs showing the light-driven transport of a 1.25 μL drop of diiodomethane up a 12° incline on the surface of a substrate organized as represented in (b). From left to right: before irradiation [pristine (*E*)-**19**], after 160 s of irradiation with UV light (just before transport), after 245 s of irradiation (just after transport), and after 640 s irradiation (photostationary state). Scale bar, 1 mm. Reproduced with permission.[95] Copyright 2005 Springer Nature.

Figure 16. (a) Structural formula of molecular rotary motor **20** employed as a dopant in liquid crystals. (b) Optical micrographs of a microscopic glass rod lying on a liquid crystalline thin film doped with 1% w/w of compound **20**. From left to right: initial state (before irradiation); top right: after 15 s of irradiation (the rod has rotated clockwise by 28°); bottom left: after 30 s (141° rotation); bottom right: after 45 s (226° rotation). Reproduced with permission.[96] Copyright 2006 Springer Nature.

Figure 17. (a) Polarized optical micrographs showing axially symmetric chiral patterns with opposite handedness (highlighted by the dashed twisted crosses), observed when a liquid crystal doped with an enantiopure molecular rotary motor and a chiral co-dopant is embedded within two closely spaced glass slides and irradiated with low intensity 375 nm light. No rotation of the patterns is observed. (b) Upon increasing the irradiation power (*P*) above a certain threshold (P_{thr}), larger and non-axisymmetric patterns are formed, which rotate continuously and unidirectionally. Both the handedness (evidenced by the dashed spirals) and the direction of rotation (marked by solid white arrows) depend on the chirality of the starting axisymmetric pattern. Scale bars, 20 μm. Adapted with permission.[102] Copyright 2018 Springer Nature.

Figure 18. (a) Schematic representation of the hierarchical self-organization of the amphiphilic molecular rotary motor **21** into nanofibers and bundles that make up macroscopic soft strings. (b) Structural formula of the molecular motor **21**. (c) Photograpic images of a supramolecular string in water subjected to UV irradiation with a source positioned on the left. Bending towards the source from 0 to 90° occurs within 60 s. Adapted with permission.[105] Copyright 2017 Springer Nature.

Figure 19. (a) Structural formula of a crosslinked polymer containing photoresponsive daisy chain units based on α-cyclodextrin hosts and azobenzene guests (one of them is highlighted in the box). The daisy chains are represented in the extended state, with the azobenzene moieties in the *E*-configuration. (b) Photographs of a square-shaped fragment of the resulting hydrogel, showing the UV light-induced shrinking and visible light-induced expansion of the material. (c) Schematic representation of the operation mechanism at the basis of the photoinduced actuation. (d) Photographs of a strip of the hydrogel suspended in water and illuminated from the right-hand side, showing the reversible bending towards the irradiation source. Adapted with permission.[108] Copyright 2016 Springer Nature.

Figure 20. (a) Structural formula of the molecular motor **22** functionalized with reactive chains, and its polymerization by Cu-AAC to generate a crosslinked polymer containing motor units. (b) Photographic snapshots of a millimeter-sized piece of gel, obtained by swelling the polymer with toluene, evidencing the shrinking caused by UV irradiation. (c) The photoinduced rotation of the molecular motor units at the branching points of the polymer determines the braiding of the chains, ultimately resulting in the contraction of the gel. Adapted with permission.[110] Copyright 2015 Springer Nature.

Figure 21. (a) Structural formula and schematic cartoon of the molecular rotary motor **23** terminated with alkyne reactive groups. (b) Structure formula of the diarylethene-based species **24** that, by a quadruple intermolecular Cu-AAC reaction with **23**, affords a crosslinked polymer that contains both molecular motor and modulator units. The open (modulator unlocked; rotation axes shown in brown) and closed (modulator locked) forms can be interconverted by UV and visible light irradiation. (c) Schematic representation of the gel obtained by co-polymerization of **23** and **24**, and of the braiding and unbraiding of its chains, induced respectively by UV and visible light irradiation. Adapted with permission.[112]

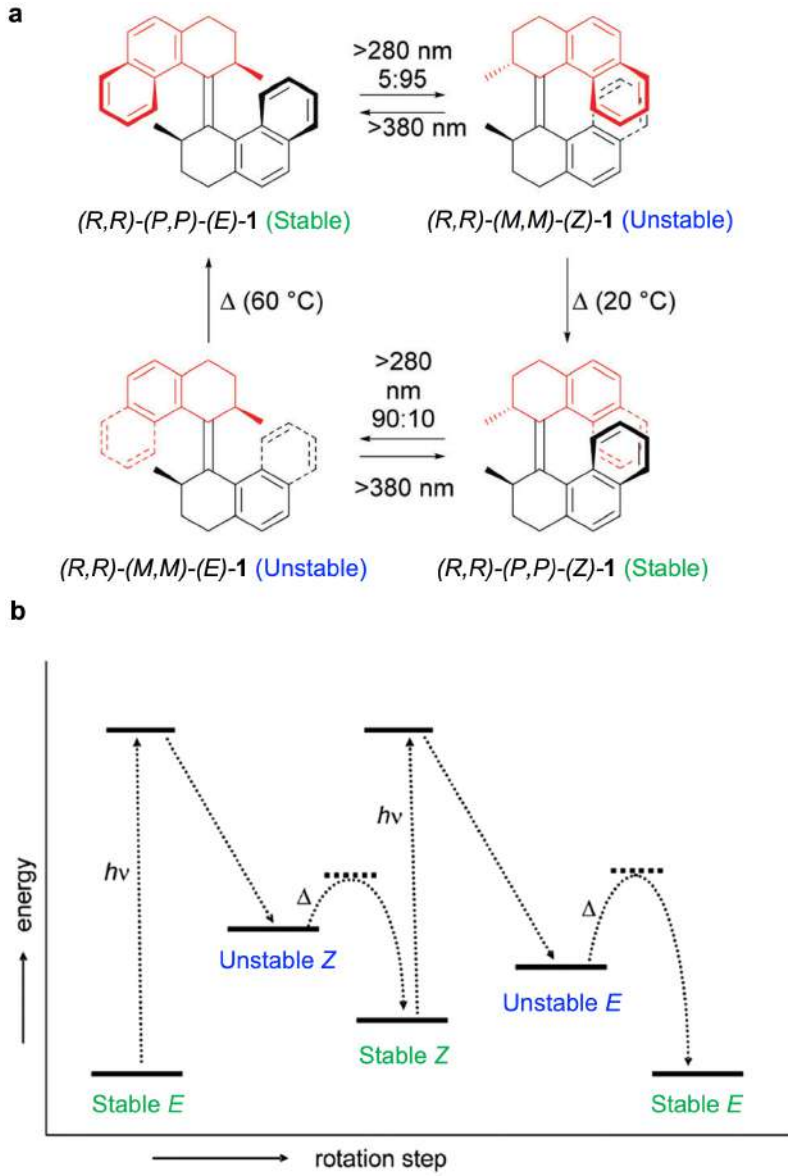
a
>280 nm
5:95
>380 nm
(R,R)-(P,P)-(E)-1 (Stable)
(R,R)-(M,M)-(Z)-1 (Unstable)
Δ (60 °C)
Δ (20 °C)
>280
nm
90:10
>380 nm
(R,R)-(M,M)-(E)-1 (Unstable)
(R,R)-(P,P)-(Z)-1 (Stable)
b
energy
hν
Δ
Unstable Z
Stable E
hν
Stable Z
Δ
Unstable E
Stable E
rotation step

Figure 1

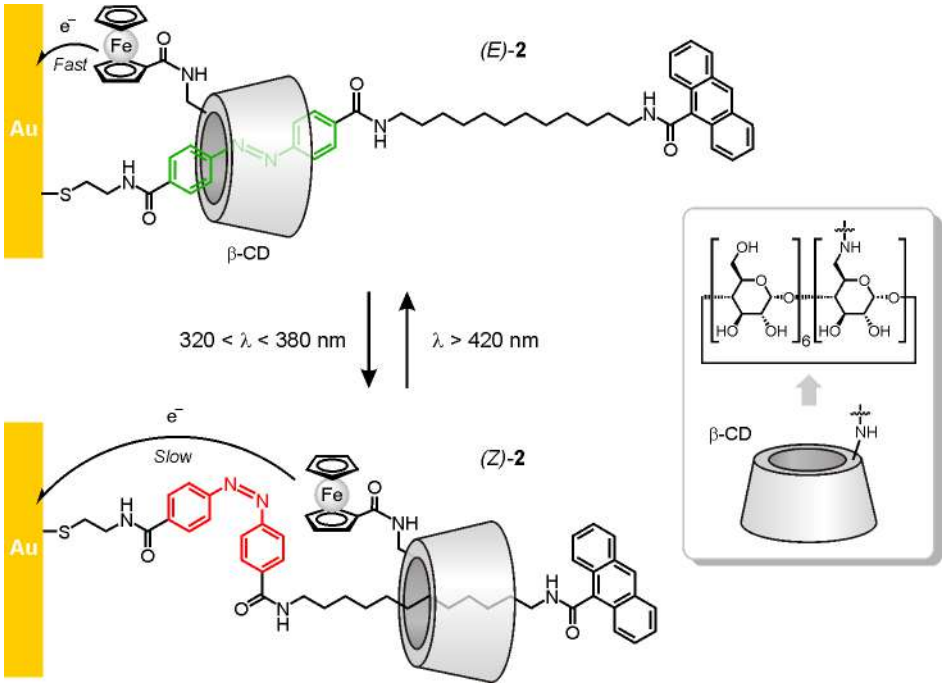

Figure 2

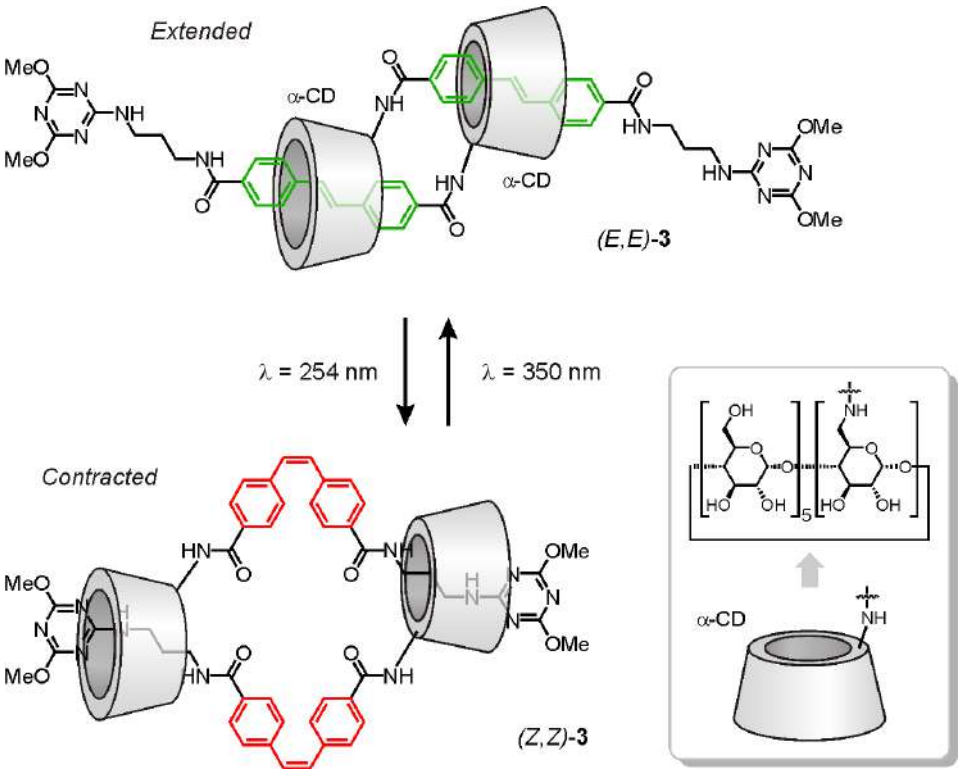

Figure 3

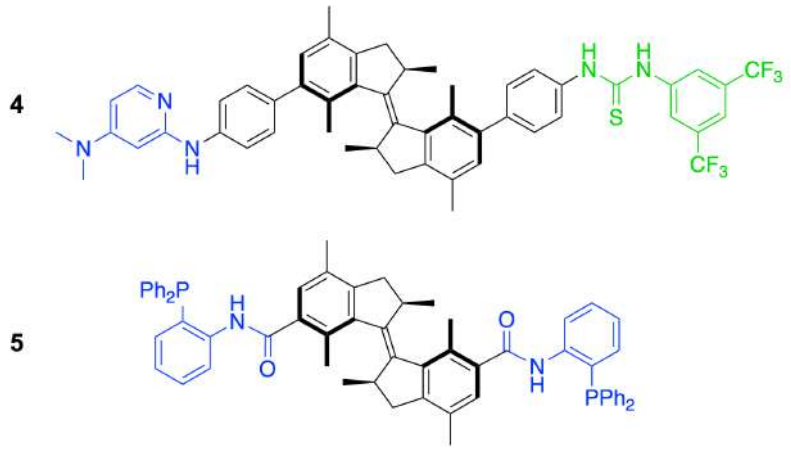

Figure 4

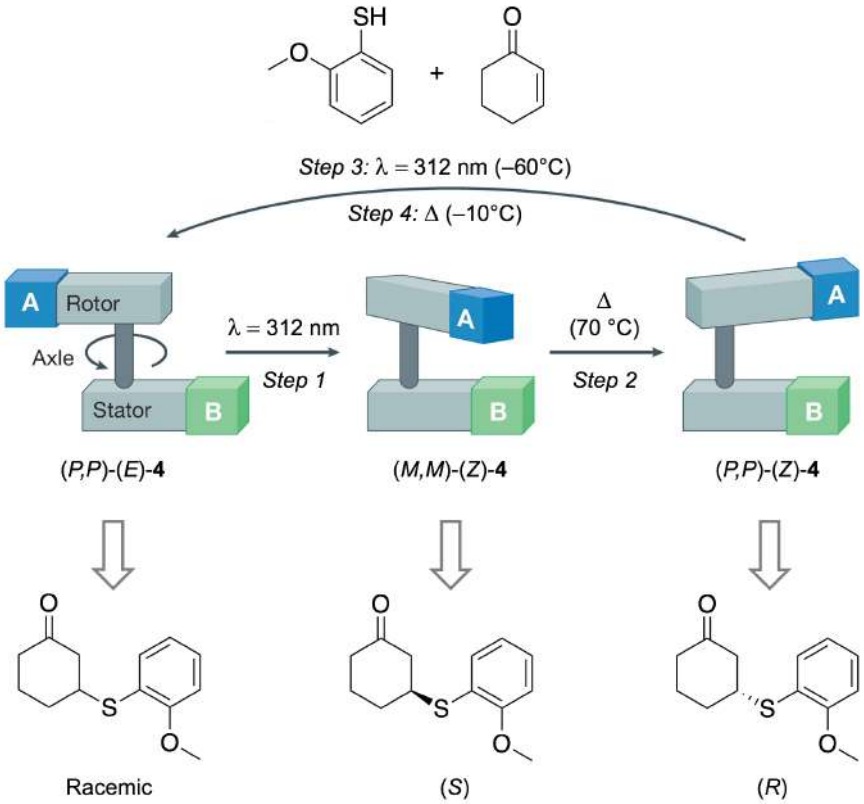

Figure 5

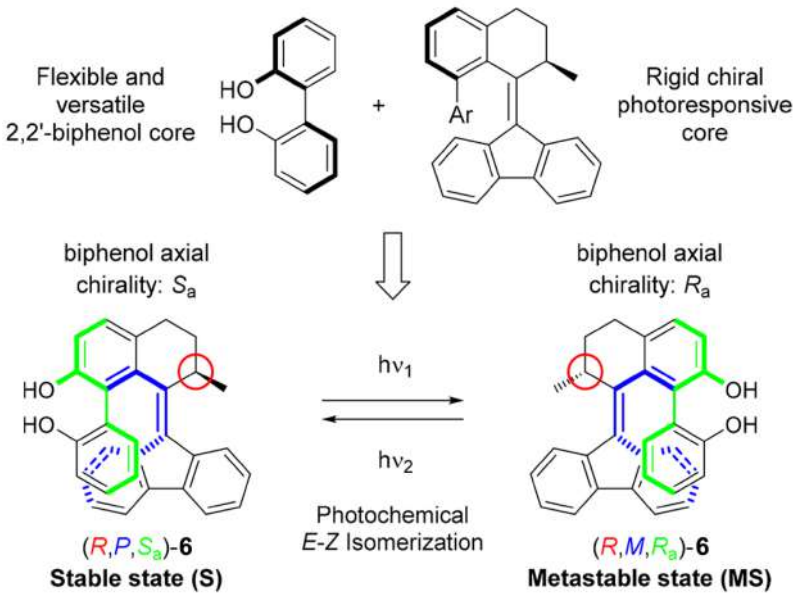

Figure 6

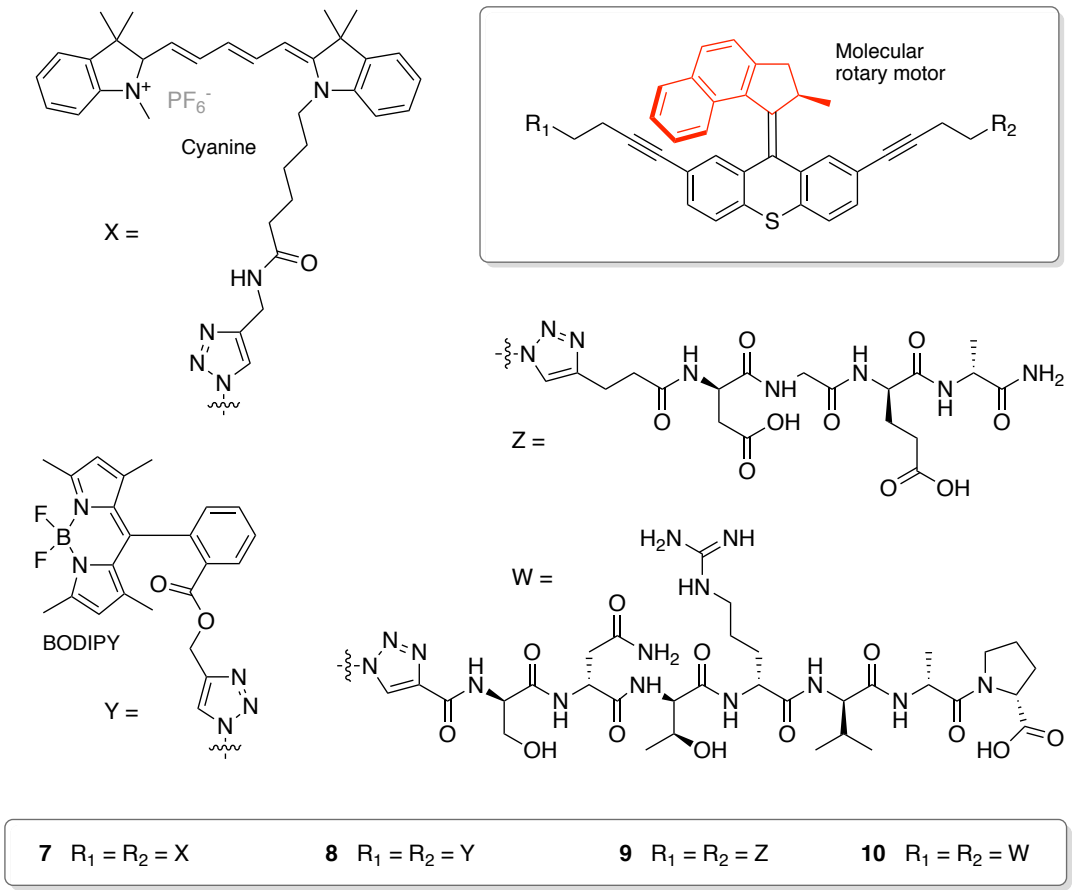

7 $R_1 = R_2 = X$ **8** $R_1 = R_2 = Y$ **9** $R_1 = R_2 = Z$ **10** $R_1 = R_2 = W$

Figure 7

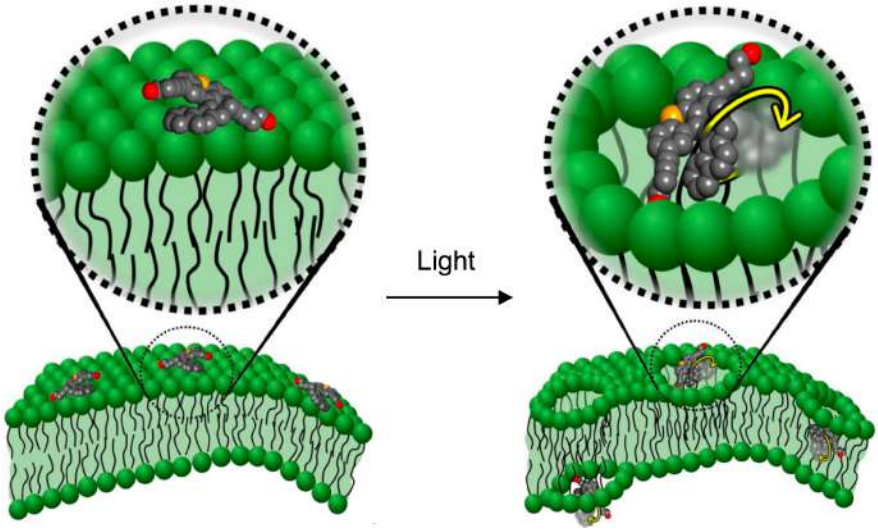

Figure 8

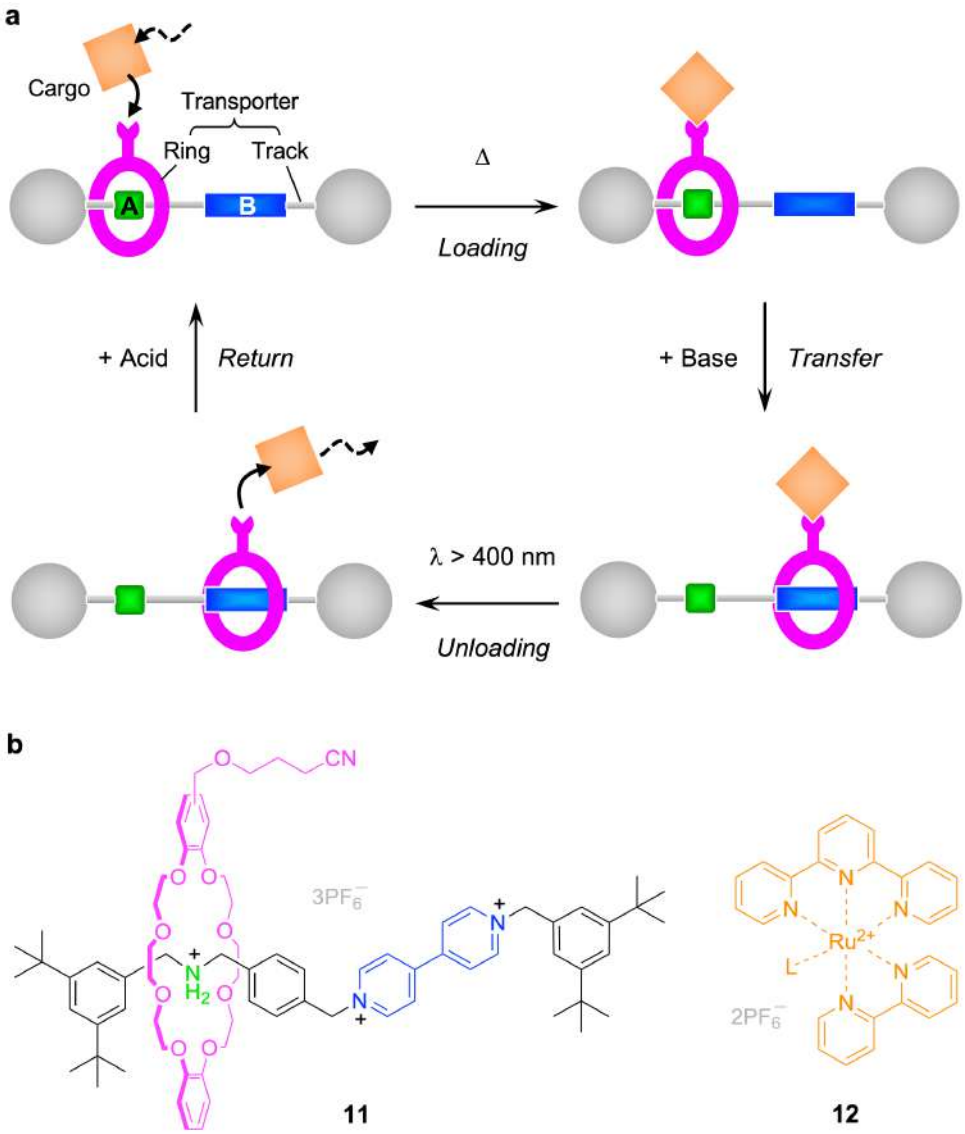
a
Cargo
Transporter
Ring
Track
A
B
Δ
Loading
+ Base
Transfer
λ > 400 nm
Unloading
+ Acid
Return
b
CN
3PF6−
11
Ru2+
2PF6−
12

Figure 9

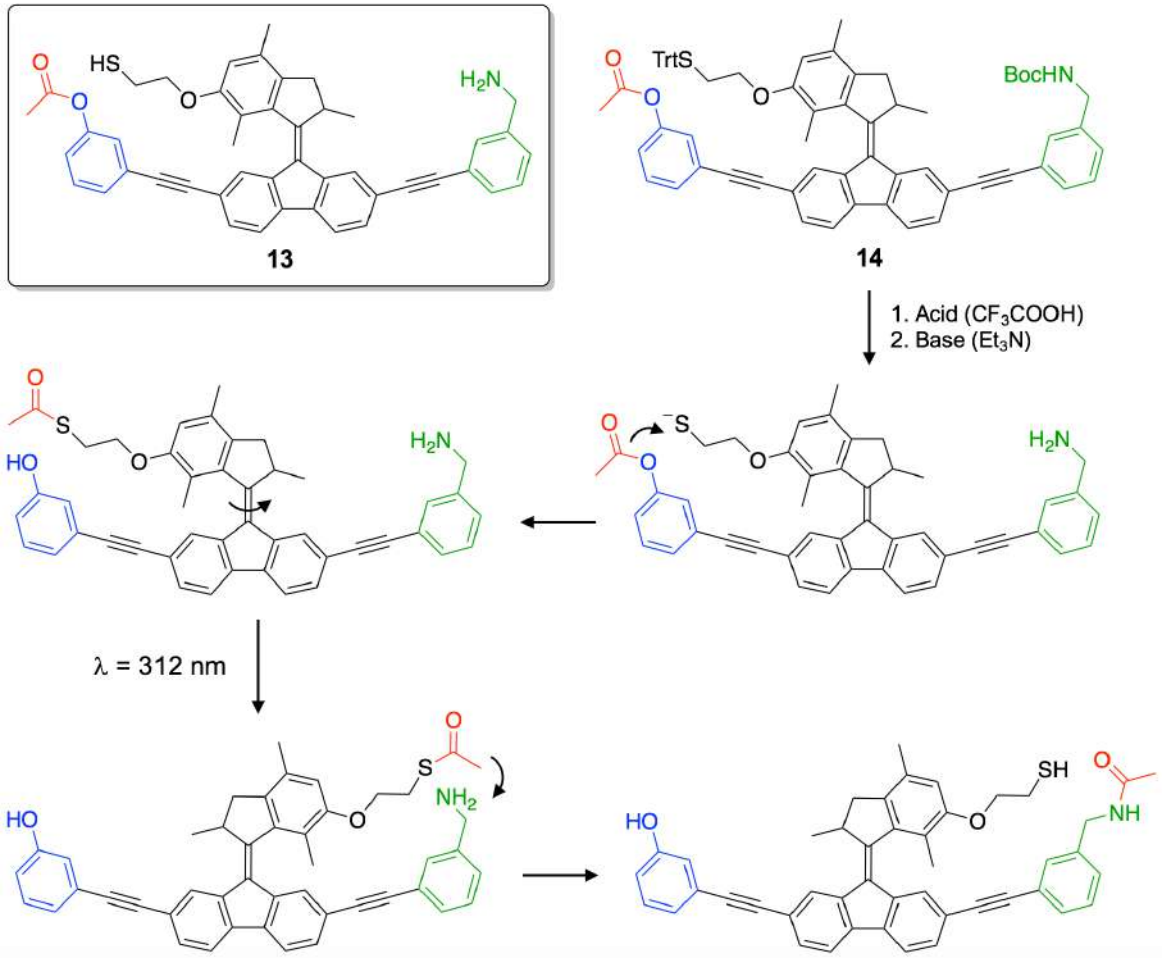
HS
O
O
H2N
13
TrtS
BocHN
14
1. Acid (CF3COOH)
2. Base (Et3N)
HO
S
NH2
λ = 312 nm
SH
NH

Figure 10

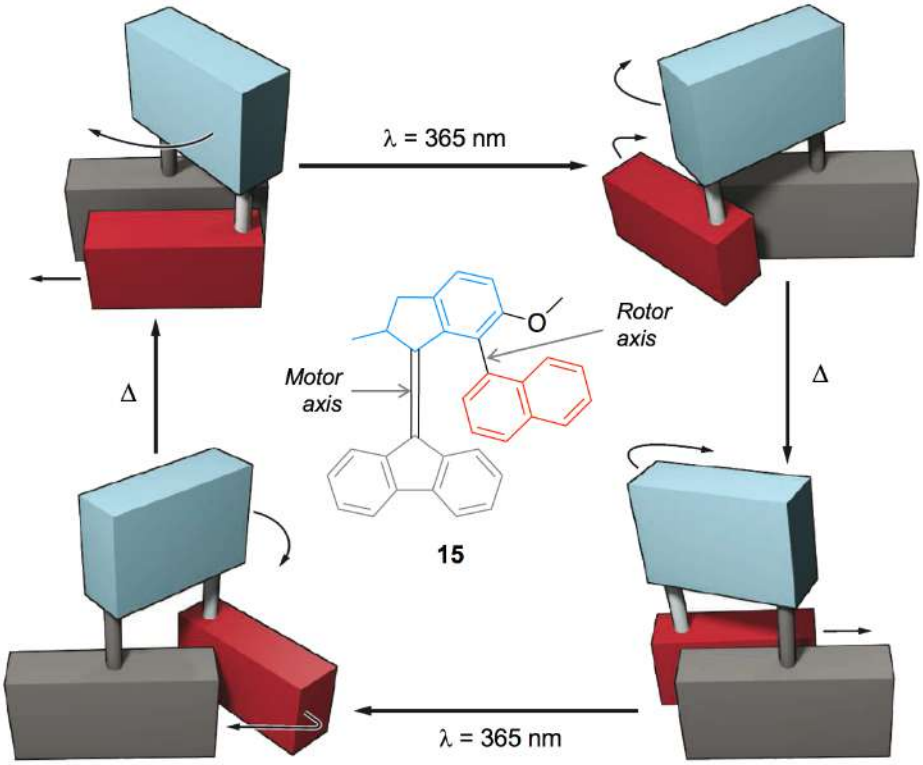

Figure 11

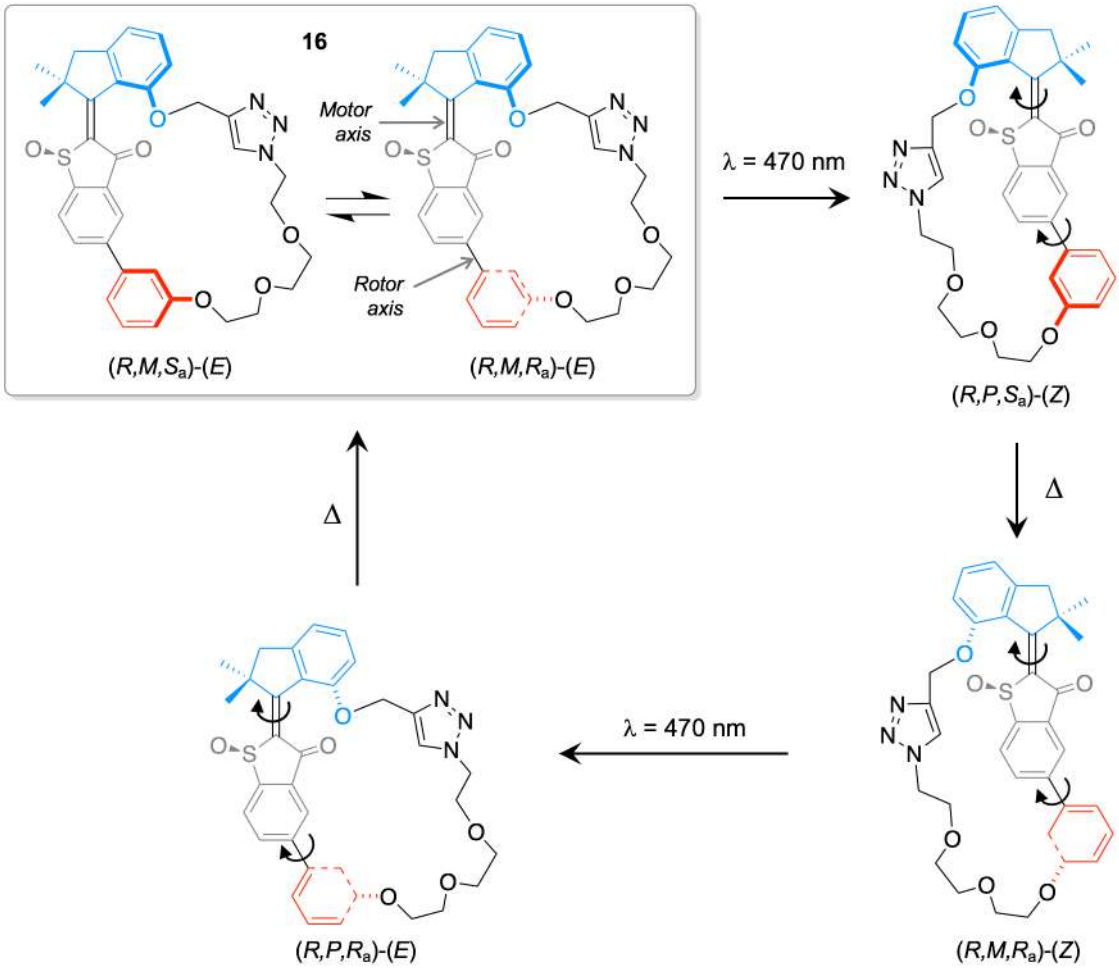
16
Motor axis
Rotor axis
(R,M,Sa)-(E)
(R,M,Ra)-(E)
λ = 470 nm
(R,P,Sa)-(Z)
Δ
(R,M,Ra)-(Z)
λ = 470 nm
(R,P,Ra)-(E)
Δ

Figure 12

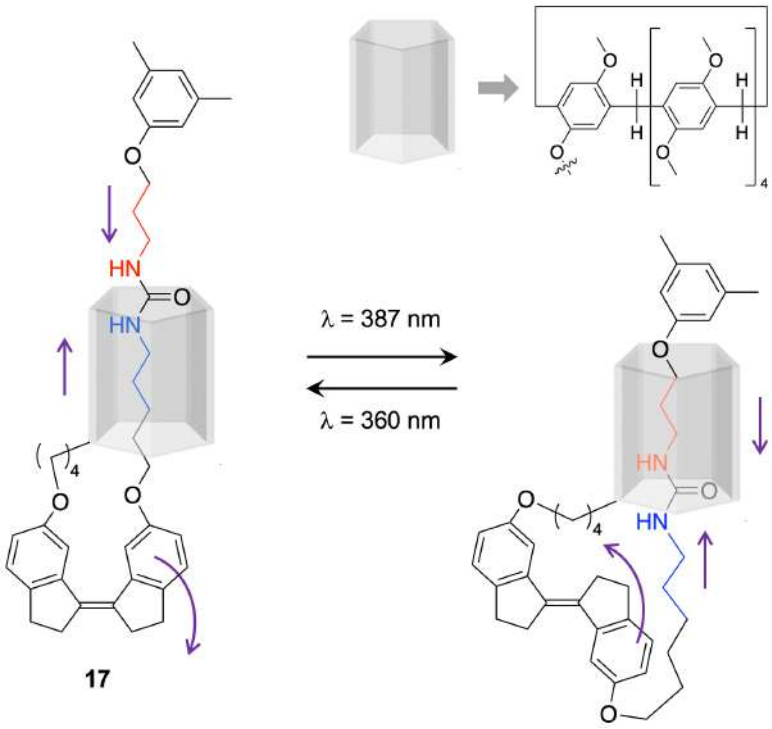

Figure 13

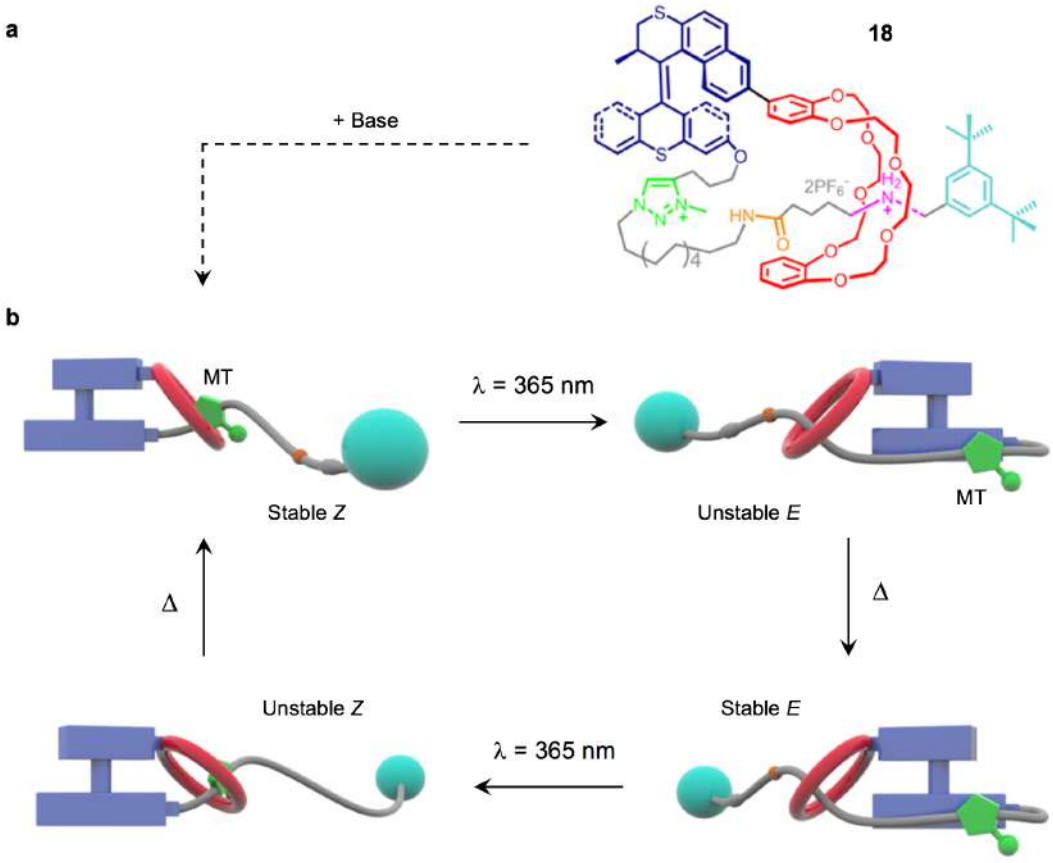
a
18
+ Base
2PF6-
b
MT
λ = 365 nm
Stable Z
Unstable E
MT
Δ
Δ
Unstable Z
Stable E
λ = 365 nm

Figure 14

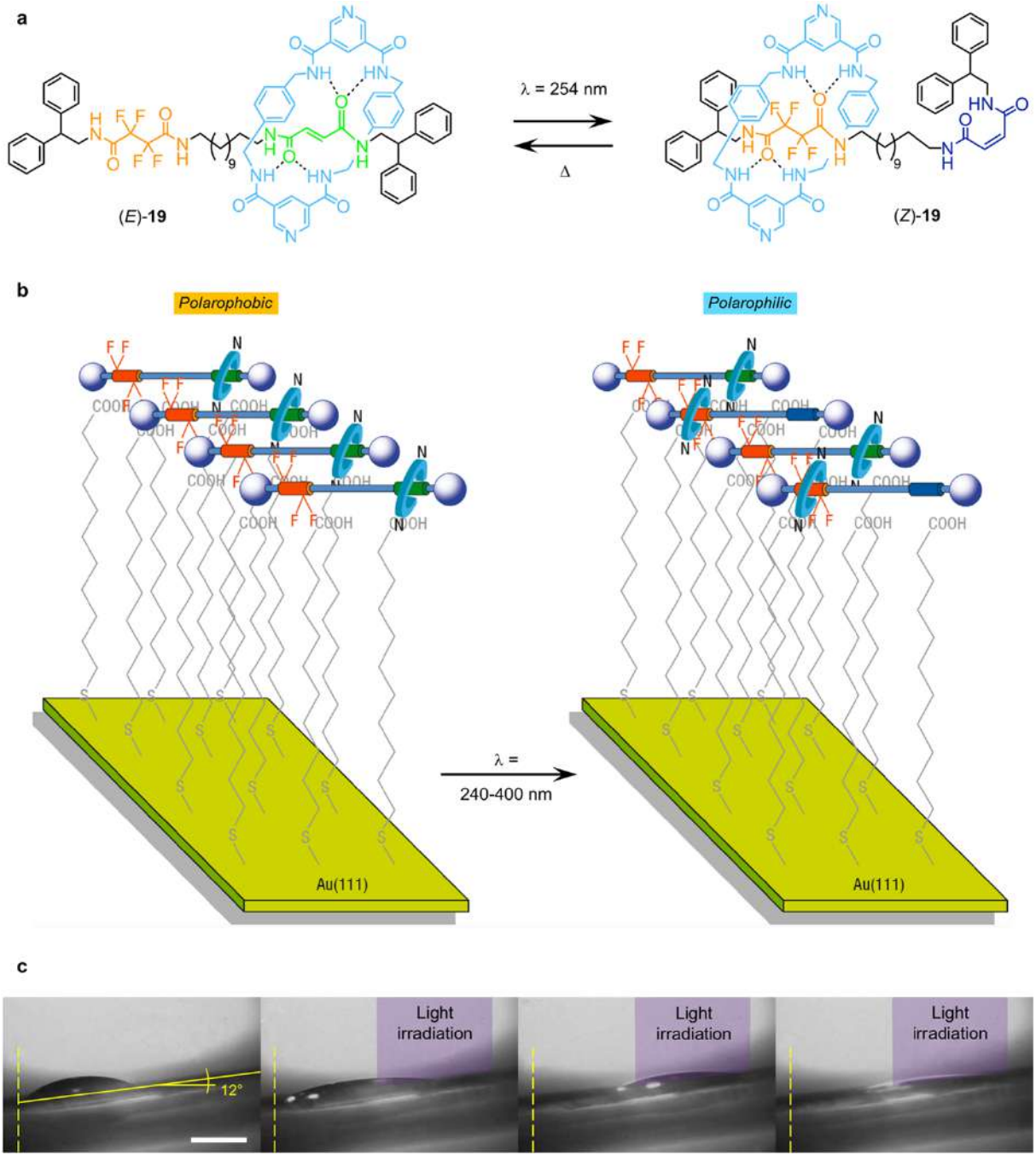

Figure 15

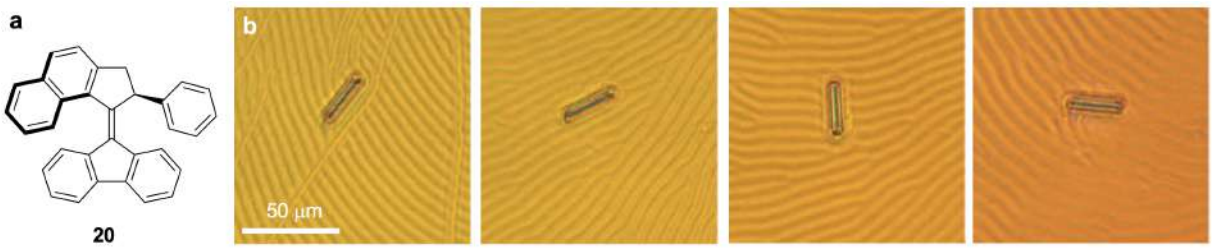

Figure 16

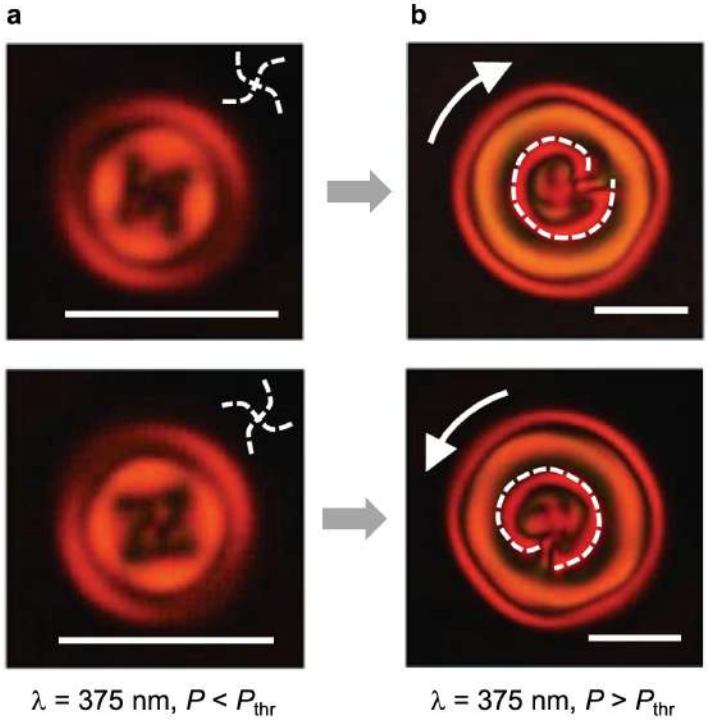

Figure 17

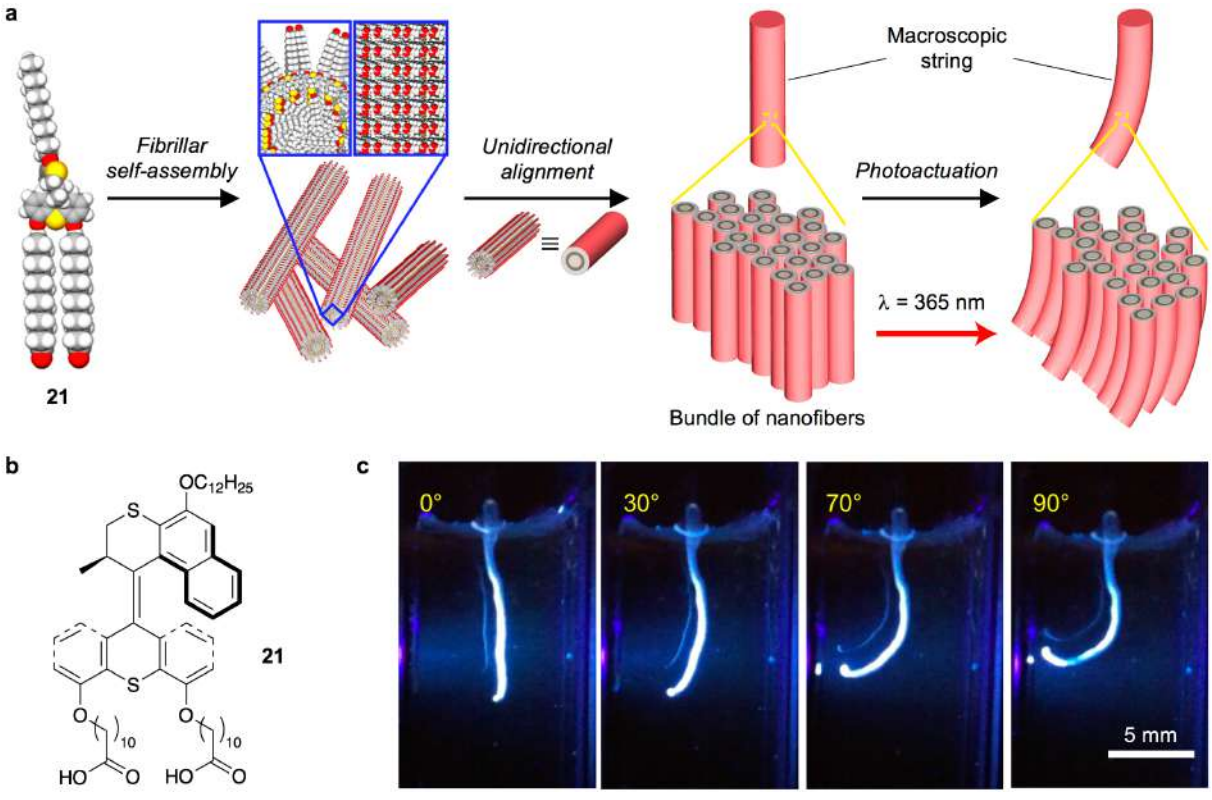

Figure 18

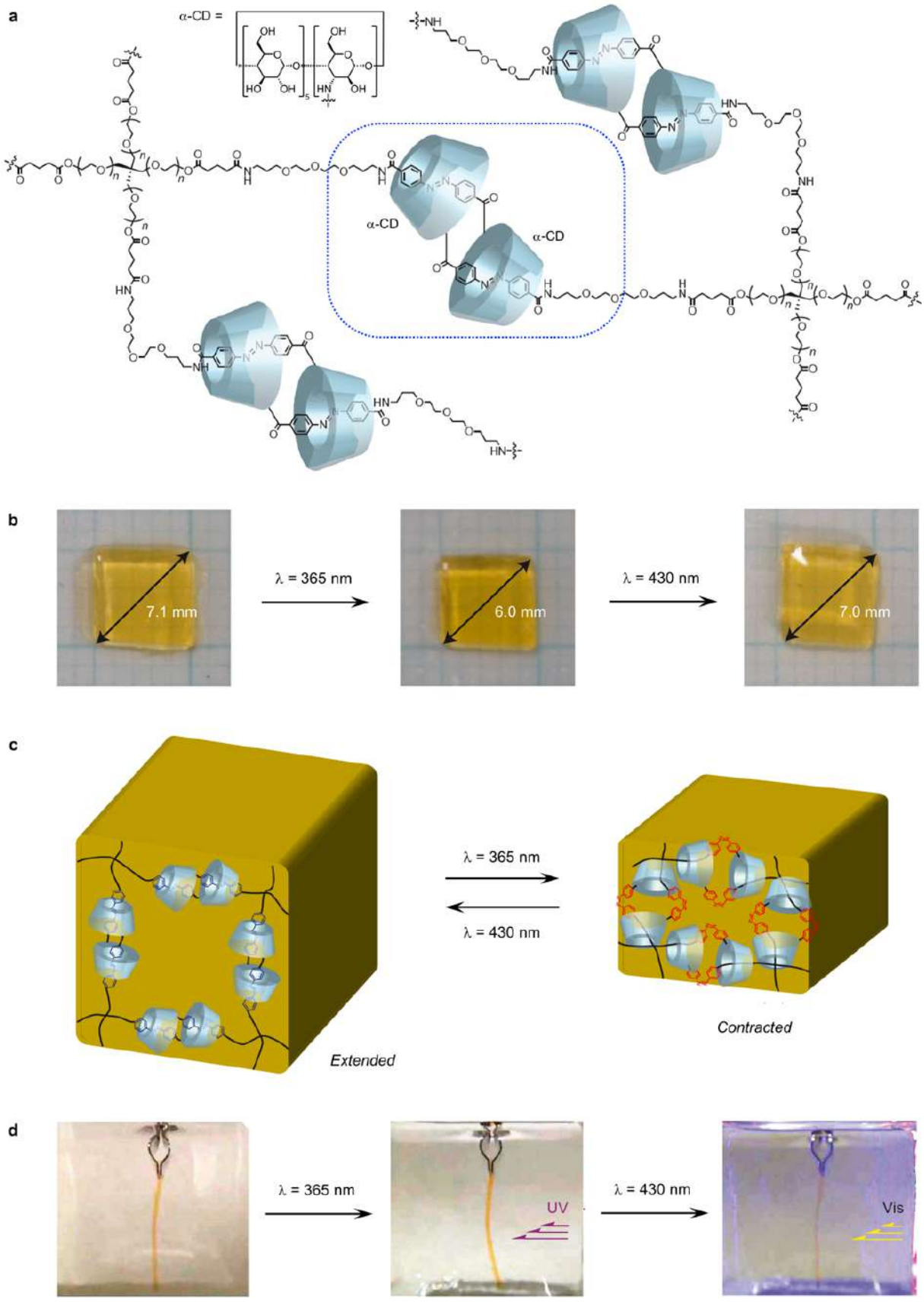
a
α-CD =
α-CD
α-CD
b
7.1 mm
λ = 365 nm
6.0 mm
λ = 430 nm
7.0 mm
c
λ = 365 nm
λ = 430 nm
Extended
Contracted
d
λ = 365 nm
UV
λ = 430 nm
Vis

Figure 19

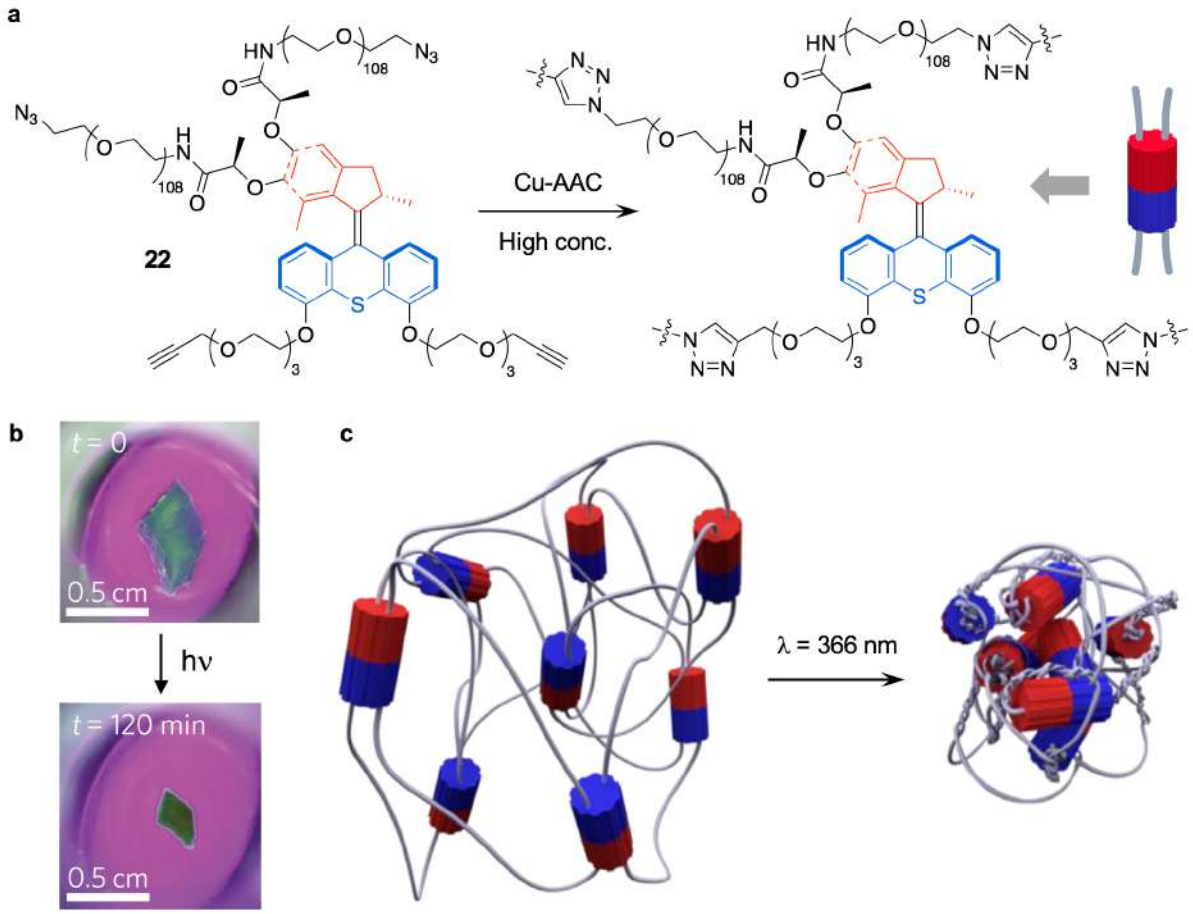

Figure 20

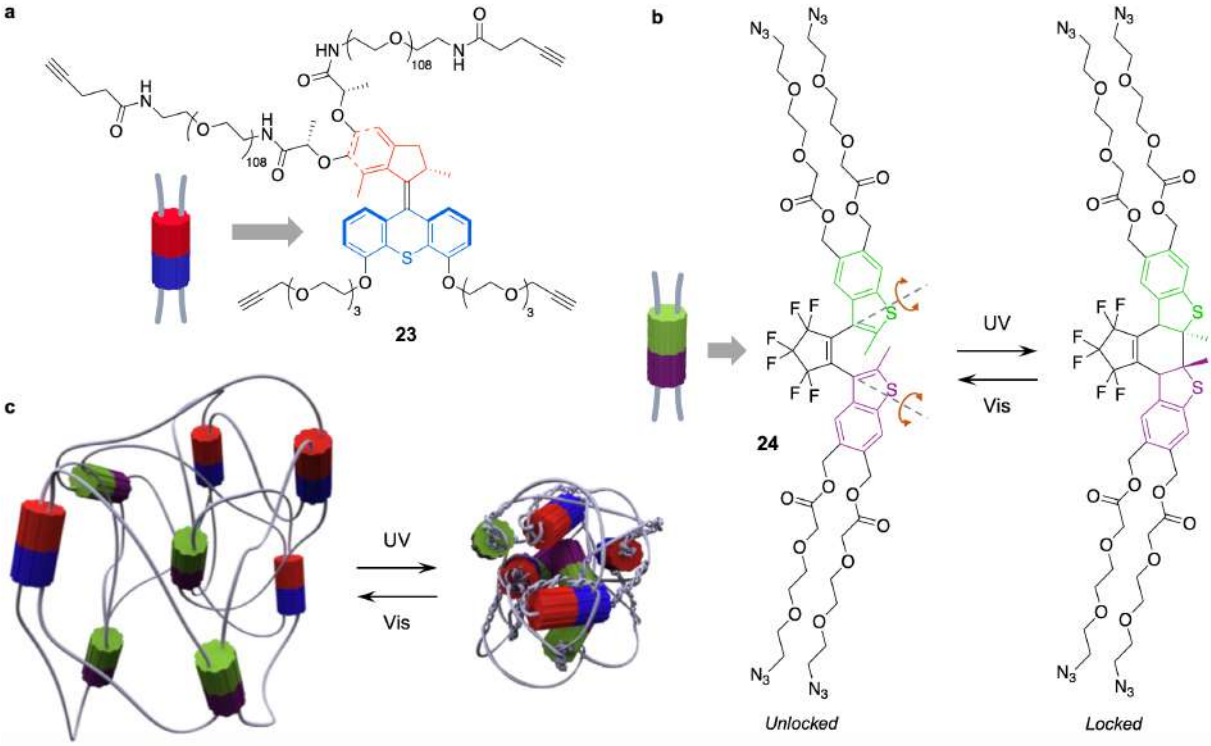

Figure 21

Three author biographies

Massimo Baroncini received his MSc in Chemistry in 2006 at the University of Bologna under the supervision of Prof. Vincenzo Balzani and his PhD in Chemical Sciences in 2010 that was awarded with the "Springer-Verlag Theses Award" in 2011. He is currently assistant professor at the University of Bologna and associate researcher at the Center for Light Activated Nanostructures (CLAN), a joint University-National Research Council laboratory. He has coauthored over 50 scientific publications, six book chapters and one monograph. His research activity deals with the synthesis and investigation of photoactive molecular and supramolecular systems and materials with tailored physico-chemical functionalities.

Serena Silvi got her MSc in 2002 at the University of Bologna with Prof. Vincenzo Balzani. In 2006 she earned her PhD under the supervision of Prof. Alberto Credi with a thesis on "Artificial Molecular Machines". From 2006 to 2008 she collaborated to the research in the Photochemistry and Supramolecular Chemistry laboratory, and since 2008 she is assistant professor at the Chemistry Department "Giacomo Ciamician" of the University of Bologna. Her research activity is focused on the design and characterization of artificial molecular machines based on interlocked structures, photochromic compounds and photoactive molecular materials, and complex systems for signal processing.

Alberto Credi is professor of Chemistry at the University of Bologna and associate research director at the National Research Council of Italy (CNR). He is the founder and director of the Center for Light Activated Nanostructures (CLAN), a joint University-CNR laboratory for research in photochemistry, supramolecular chemistry, materials science and nanoscience. His research deals with the development of stimuli responsive molecular-based systems, with a particular focus on logic devices, machines and motors. He has authored four books and over 280 scientific publications, and he is the PI of an ERC Advanced Grant for the development of light driven molecular motors.

Table of contents entry: Artificial molecular machines powered by light can nowadays be integrated in organized environments such that the molecular movements can be harnessed to execute a task. The resulting functional devices and materials can lead to radical innovation in catalysis, microfluidics soft robotics, medical diagnostics and therapy, and solar energy conversion.

Keyword: nanotechnology

S. Corra, M. Curcio, M. Baroncini, S. Silvi and A. Credi*

Photo-activated artificial molecular machines that can perform tasks